The Circadian Clock Gene BMAL1 Coordinates Intestinal Regeneration

cmgh
CELLULAR AND MOLECULAR GASTROENTEROLOGY AND HEPATOLOGY

ORIGINAL RESEARCH

The Circadian Clock Gene *BMAL1* Coordinates Intestinal Regeneration

Kyle Stokes,[1] Abrial Cooke,[1] Hanna Chang,[1] David R. Weaver,[2] David T. Breault,[3,4,5,a] and Phillip Karpowicz[1,a]

[1]Department of Biological Sciences, University of Windsor, Windsor, Ontario, Canada; [2]Department of Neurobiology, University of Massachusetts Medical School, Worcester, Massachusetts; [3]Harvard Stem Cell Institute, Cambridge, Massachusetts; [4]Division of Endocrinology, Boston Children's Hospital, Boston, Massachusetts; [5]Department of Pediatrics, Harvard Medical School, Boston, Massachusetts

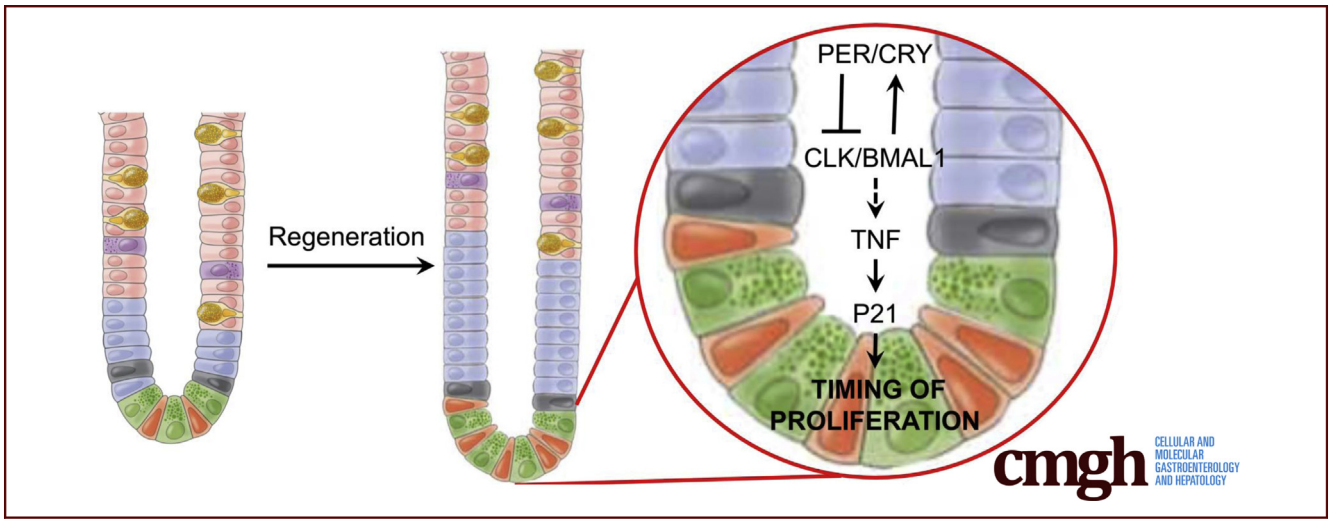

SUMMARY

We investigated the circadian timing of intestinal regeneration using the null mutant BMAL1. Our results show that the circadian clock regulates the timing of inflammation and proliferation during regeneration.

BACKGROUND & AIMS: The gastrointestinal syndrome is an illness of the intestine caused by high levels of radiation. It is characterized by extensive loss of epithelial tissue integrity, which initiates a regenerative response by intestinal stem and precursor cells. The intestine has 24-hour rhythms in many physiological functions that are believed to be outputs of the circadian clock: a molecular system that produces 24-hour rhythms in transcription/translation. Certain gastrointestinal illnesses are worsened when the circadian rhythms are disrupted, but the role of the circadian clock in gastrointestinal regeneration has not been studied.

METHODS: We tested the timing of regeneration in the mouse intestine during the gastrointestinal syndrome. The role of the circadian clock was tested genetically using the *BMAL1* loss of function mouse mutant *in vivo*, and *in vitro* using intestinal organoid culture.

RESULTS: The proliferation of the intestinal epithelium follows a 24-hour rhythm during the gastrointestinal syndrome. The circadian clock runs in the intestinal epithelium during this pathologic state, and the loss of the core clock gene, *BMAL1*, disrupts both the circadian clock and rhythmic proliferation. Circadian activity in the intestine involves a rhythmic production of inflammatory cytokines and subsequent rhythmic activation of the JNK stress response pathway.

CONCLUSIONS: Our results show that a circadian rhythm in inflammation and regeneration occurs during the gastrointestinal syndrome. The study and treatment of radiation-induced illnesses, and other gastrointestinal illnesses, should consider 24-hour timing in physiology and pathology. *(Cell Mol Gastroenterol Hepatol 2017;4:95–114; http://dx.doi.org/10.1016/j.jcmgh.2017.03.011)*

Keywords: Intestine; Circadian Rhythms; Gastrointestinal Syndrome; TNF; Intestinal Stem Cells.

[a]Authors share co-senior authorship and contributed equally.

Abbreviations used in this paper: LD, light/dark; NFκB, nuclear factor κB; PBS, phosphate-buffered saline; pHH3, phosphorylated histone H3; pJUN, phosphorylated c-JUN; TNF, tumor necrosis factor; ZT, Zeitgeber time.

Most current article

2352-345X
http://dx.doi.org/10.1016/j.jcmgh.2017.03.011

See editorial on page 203.

The intestinal epithelium can produce cells at a prodigious rate, and a long-standing question in the field is what mechanisms underlie its regeneration following damage or stress. The epithelium is maintained by a population of stem cells that divide to produce transit-amplifying precursors, differentiated enterocytes, goblet cells, Paneth cells, and enteroendocrine cells.[1] Stem cells and precursors are localized to the base of the crypts of Lieberkühn, and their progeny differentiate as they move upward toward the villus. The use of radiation to damage the epithelium and initiate a regenerative response is an important and clinically relevant model to study regeneration in the small intestine.[2,3]

High levels of radiation induce the gastrointestinal syndrome,[4–6] an illness associated with the loss of dividing precursors and stem cells during the first 24 hours, and breakdown of the epithelial barrier, which leads to increased permeability, infection, and extensive inflammation.[6] This is then followed by a regenerative response initiated from a surviving population of stem cells. Understanding the mechanisms underlying the gastrointestinal syndrome provides essential insight into intestinal regeneration, with the potential for impacting patients exposed to ionizing radiation.

The timing of the molecular and cellular mechanisms, or chronobiology, of the gastrointestinal syndrome is poorly understood. In general, the importance of intestinal chronobiology is somewhat underappreciated, although 1 form of timing, its circadian rhythms, has been studied extensively.[7] Circadian rhythms are biologic processes that occur with an approximate cycle of 24 hours. They are driven by a highly conserved molecular pacemaker, called the circadian clock, which produces 24-hour rhythms in animal behavior and physiology.[8] An example of a circadian rhythm is an animal's locomotor activity; when the clock is disrupted, activity becomes arrhythmic.[9]

In mammals, the circadian clock consists of the transactivators *CLK* and *BMAL1* (also called *ARNTL*) and their negative regulators *PER1-3* and *CRY1-2*.[8,10] The transcriptional targets of CLK/BMAL1 include *PER1-3* and *CRY1-2*, which accumulate as proteins during the night to repress their own expression. A second form of transcriptional control is driven by *RORα* and *REV-ERBα* (also called *NR1D1*) that activate and repress *BMAL1* expression, respectively. Posttranscriptional and posttranslational mechanisms also contribute to rhythmicity.[11] Photoperiod, ingested food, and hormone levels synchronize circadian clocks throughout the body to drive 24-hour transcriptional rhythms with characteristic maxima and minima at specific times of day. A tremendous number of processes throughout the body are influenced by the circadian clock. For example, more than 40% of the genome is expressed rhythmically, and in different tissues 3%–16% of these genes are rhythmic, and include key rate-limiting enzymes.[12] Previous studies have shown that circadian transcriptional rhythms are present in the digestive tract,[13–16] but their function has not been tested.

Circadian rhythms are important in human health and, in particular, influence several digestive system illnesses. Shift-workers undergo photoperiod disruption and experience higher rates of gastrointestinal pain,[17] ulcers,[18] and colorectal cancer.[19] Experimental models also reveal that colitis is worsened during photoperiod disruption,[20] highlighting a possible connection between circadian rhythms and intestinal inflammation. The response to gastrointestinal injury is also time-dependent: patients with cancer treated with radiotherapy have more severe intestinal mucositis when irradiated in the morning versus in the evening.[21] These studies show that digestive tract physiology changes according to time of day, and that disruption to this timing has negative consequences.

Although circadian rhythms are widespread throughout the body, the circadian timing system is hierarchical.[22] A circadian clock in the suprachiasmatic nucleus of the hypothalamus receives light input from the retina to synchronize it to the daily light/dark (LD) cycle. Even in the absence of light input, the suprachiasmatic nucleus generates rhythms in body temperature, food intake, and hormone levels that synchronize circadian clocks in other tissues, such as the intestine, which normally receive synchronizing information originating in the brain. To what extent does the intrinsic clock in the intestine regulate the regenerative response? Despite data showing circadian rhythms in the intestine and the immune system, studies of gastrointestinal disease do not consider time-of-day effects.

To address this fundamental question we investigated the timing of intestinal regeneration in the epithelium of mice with the gastrointestinal syndrome, and found diurnal rhythms in crypt cell proliferation. We next investigated the role of the core circadian clock gene, *BMAL1*, in the intestine before and after acute radiation injury. Regeneration in this tissue is *BMAL1*-dependent, which regulates daily timing of the JNK stress response pathway activity and subsequent proliferation. Our data suggest that cytokines, which are rhythmically expressed in the intestine during regeneration, drive a circadian stress response in the epithelium. By regulating the stress response, *BMAL1* promotes the 24-hour rhythmic production of intestinal epithelia. These data shed light on the importance of the circadian clock during intestinal illness and regeneration.

Materials and Methods

Animal Housing

BMAL1$^{+/+}$ and *BMAL1*$^{-/-}$ mouse littermates were bred from *BMAL1*$^{+/-}$ parents (Jackson Laboratories, Bar Harbor, ME #009100), and were housed on a 12-hour light/12-hour dark photoperiod with *ad libitum* food. We use the term diurnal, rather than circadian, in the text because all of our experiments were performed on a LD photoperiod, rather than in the absence of circadian entrainment factors. All mice were maintained according to animal care regulatory approval at Boston Children's Hospital (#A07 09 124R), University of Massachusetts Medical School (#A-1315), or

the University of Windsor (#AUPP 14-21). Gamma irradiation was performed at Zeitgeber time (ZT) 3 at 1.05 Gy/min for a total of 12 Gy in 1 single treatment, and animals were returned to 12-hour light/12-hour dark photoperiod with *ad libitum* food, and Bactrim antibiotic (Hi Tech Pharmacal, Amityville, NY) in drinking water following treatment. Intestinal tissues were sampled from irradiated mice, or control (undamaged) animals housed under the same LD photoperiod conditions, at Day 4, for 24 hours following irradiation. A total of 3–4 mice were examined per condition (normal conditions vs irradiation, genotype, time point). Both female and male mice were included in the study, because no significant sex-linked differences were found in all of the parameters examined in this study.

Intestinal Tissues

Animals were humanely euthanized using CO_2 at 4-hour time points over a day: ZT0, ZT4, ZT8, ZT12, ZT16, and ZT20 as indicated in Figures 1–9. For data shown in Figure 1*B*, tissue was collected at Day 0, 1, 2, 3, 4, and 5 at ZT4. Samples of proximal intestine (10 cm of small intestine containing duodenum and a portion of the jejunum) were collected for analysis. Samples were flushed clean using 4 mM sodium phosphate buffer pH7.4 + 155 mM saline (phosphate-buffered saline [PBS]). Each 10-cm sample was further cut into 4–5 segments. A ~0.5-cm portion of each 2-cm segment was collected in RNAlater buffer (Qiagen, Toronto, Ontario, Canada) and stored at -80°C for RNA purification. The remaining ~1.5-cm segments of intestine were fixed in 4% paraformaldehyde (Electron Microscopy Sciences, Hatfield, PA) + PBS overnight at 4°C for immunofluorescence and histology.

RNA Purification and Analysis

In vivo tissue was homogenized in RLT Buffer (Qiagen) using a Bullet Blender (Next Advance, Averill Park, NY) according to the manufacturer's protocol. Organoids (see later) were lysed directly into RLT Buffer and vortexed until the solution was homogenous. RNA was purified using the RNEasy Mini RNA purification kit (Qiagen), and RNA was then transcribed to cDNA using the iScript RT Supermix (Bio-Rad, Mississauga, Ontario, Canada) according to the manufacturer's protocols.

Quantitative Polymerase Chain Reaction

cDNA levels were quantified using the iTaq Universal SYBR Green Supermix (Bio-Rad) on a Viia7 real-time polymerase chain reaction system (Thermo Fisher Scientific). From 3–4 samples were examined per genotype, at each time point or condition (see previous sections for details of tissue collection and RNA purification). Primer sequences were obtained from PrimerBank, and amplified at ~90% efficiency. The primers used are shown in Table 1.

Immunofluorescence and Histochemistry

Following fixation, intestinal tissues were washed in PBS three times and immersed in 30% sucrose + PBS overnight at 4°C to cryoprotect. Tissues were mounted in Tissue-Tek O.C.T compound (Sakura, Flemingweg, Netherlands) and sectioned at 10-μm thickness on a cryostat. Slides containing tissue sections were washed 3 times for 5 minutes at room temperature with PBS. Organoids were stained in 1.5-mL microcentrifuge tubes following fixation. Samples were blocked using 5% normal goat serum (Thermo Scientific, Toronto, Ontario, Canada) in PBS + 0.3% Triton-X100 (Fisher, Toronto, Ontario, Canada) for 1 hour. Primary antibody was applied overnight (anti-Villin 1:1000, anti Lysozyme 1:1000, anti-CCL2 1:75 [Abcam, Toronto, Ontario, Canada ab130751, ab108508, ab8101, respectively]; anti-Ki67 1:500 [Vector Labs VP-RM04]; anti-Phospho-HistoneH3 [Ser 10] 1:1000 [Upstate/Millipore, Etobicoke, Ontario, Canada 06-570]; anti-Per2 1:200 [Millipore AB5428P]; anti–nuclear factor κB [NFκB] 1:400, anti-Phospho-c-Jun S73 1:800 [Cell Signaling Technology B14E12, D47G9, respectively]; anti-GFP 1:2000 [Nacalai Tesque Inc., Kyoto, Japan GF090R]; anti-cleaved Caspase3 1:200 [Cell Signaling Technology 9661s] in 1.2% normal goat serum at 4°C overnight. Sections were washed in PBS 3 times for 5 minutes followed by incubation in Alexa 488, or Alexa 555 (Life Technologies, Toronto, Ontario, Canada) secondary antibodies for 1 hour (1:2000), and counterstained with DAPI or TOPRO3 nuclear stains (Life Technologies) in 1.2% normal goat serum at room temperature. Sections were then washed 3 times for 5 minutes in PBS at room temperature and mounted using Prolong Antifade Gold (Invitrogen, Toronto, Ontario, Canada). Antigen retrieval was performed for CCL2, Lysozyme, NFκB, and Ki67 using sodium citrate buffer + 0.5% Tween for 10 minutes at 109°C, 1.7 PSI. Antigen retrieval was performed for PER2, GFP, and Phospho-c-Jun using 1% sodium dodecyl sulfate for 10 minutes at room temperature. EdU staining was done using the Click iT EdU Alexafluor 555 kit according to manufacturer's instructions (Thermo Scientific). Alcian blue (EMS) staining was done at 30 minutes, room temperature. The sections were washed under running water for 2 minutes then immediately rinsed with distilled water. The sections were then counterstained with Nuclear Fast Red (EMS) for 5 minutes at room temperature. Sections were dehydrated in 95% ethanol 2 times for 5 minutes at room temperature, followed by another dehydration step with 100% ethanol 2 times for 5 minutes at room temperature. Sections were cleared using Histo-clear (EMS) 2 times for 10 minutes at room temperature, and mounted in Clearium (EMS). A total of 3–4 samples were examined per condition (normal conditions versus irradiation, genotype, time point).

Microscopy and Quantification

Organoid images were taken using a Keyence BZ9000 microscope. Intestinal tissue sections were imaged using either a Olympus Fluoview FV-1000 confocal microscope or a Zeiss LSM780 confocal microscope. Images were processed using Adobe Photoshop CS5. Antibody-positive cells were quantified as the total number of labeled cells/total number of DAPI+ nuclei present in a crypt section. Twenty crypts were sampled per animal for the quantification of Ki67, phosphorylated histone H3 (pHH3),

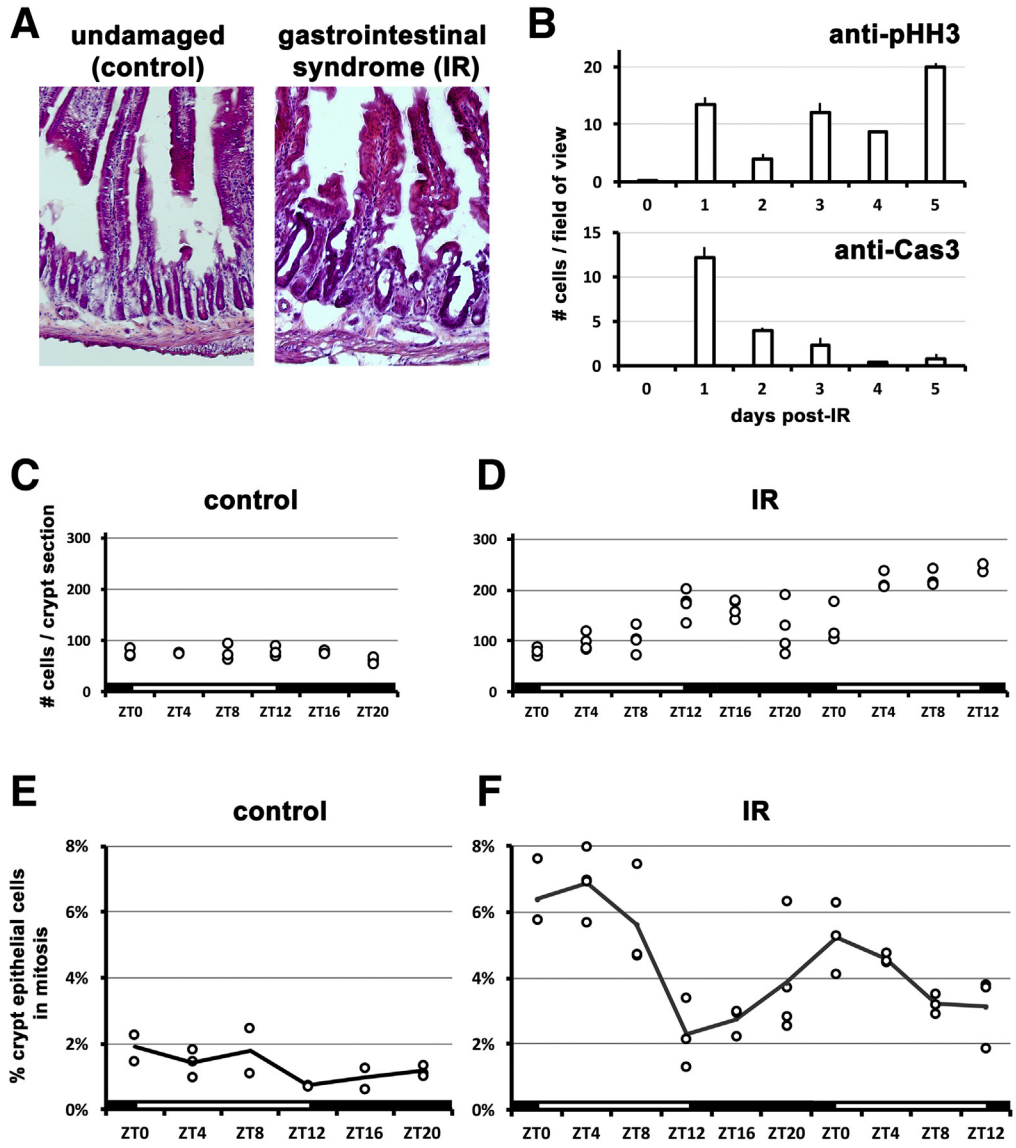

Figure 1. Cell proliferation exhibits a diurnal rhythm during the gastrointestinal syndrome. (*A*) Crypts exhibit changes following irradiation (IR), during the gastrointestinal syndrome (4 days after IR). Hematoxylin-eosin staining shows villus morphology is disrupted, and crypts are less abundant, larger, and hyperplastic. (*B*) Proliferation and cell death timing over 5 days following IR was assessed in the morning. After injury, proliferation (marked by antiphosphorylated Histone H3 mitoses) increases, whereas cell death (marked by anticleaved Caspase3 apoptosis) decreases. (*C*) In the control (nonirradiated) state, crypt nuclei number is constant ($P = .3669$). Each data point represents the average of 1 animal (20 crypts sampled). ZT on the x-axis refers to the time lights turn on (ZT0) and off (ZT12). (*D*) Following IR, the number of cells increases over 36 hours between Days 4 and 6 of healing ($F = 10.53$; $P < .0001$). This is likely a result of increased proliferation as the epithelium repairs itself from IR damage. (*E*) Mitoses in the control (nonirradiated) are constant without significant differences over time ($P = .2909$). (*F*) During the gastrointestinal syndrome (IR), mitoses exhibit a strong diurnal rhythm with significant differences at different times ($F = 11.32$; $P < .0001$). Mitoses peak at approximately ZT0-4 over both days. Each *data point* represents the average of 1 animal (20 crypts sampled), and the *solid line* indicates the average of these.

phosphorylated c-JUN (pJUN), Caspase3, or FUCCI reporters, with 3–4 animals/organoid lines examined per condition. Paneth cells were quantified as the number of lysozyme-positive cells per crypt in 30 crypts sampled from 3 animals of each genotype. Goblet cells were quantified as the number of alcian blue–positive cells in 10 villi field of views (×20 objective) per animal from 3 animals of each genotype. Crypts were counted by sampling 10 regions of 1 mm from 6 animals of each genotype. Quantification of data shown in Figures 1*B*, 2*A*, 3*A*, and 3*C* was done at the time point ZT4.

Statistics

Statistical analysis was carried out using Student's *t* test to compare genotype differences (Figures 1*A*, 2*A*, 3*A*, 3*D*,

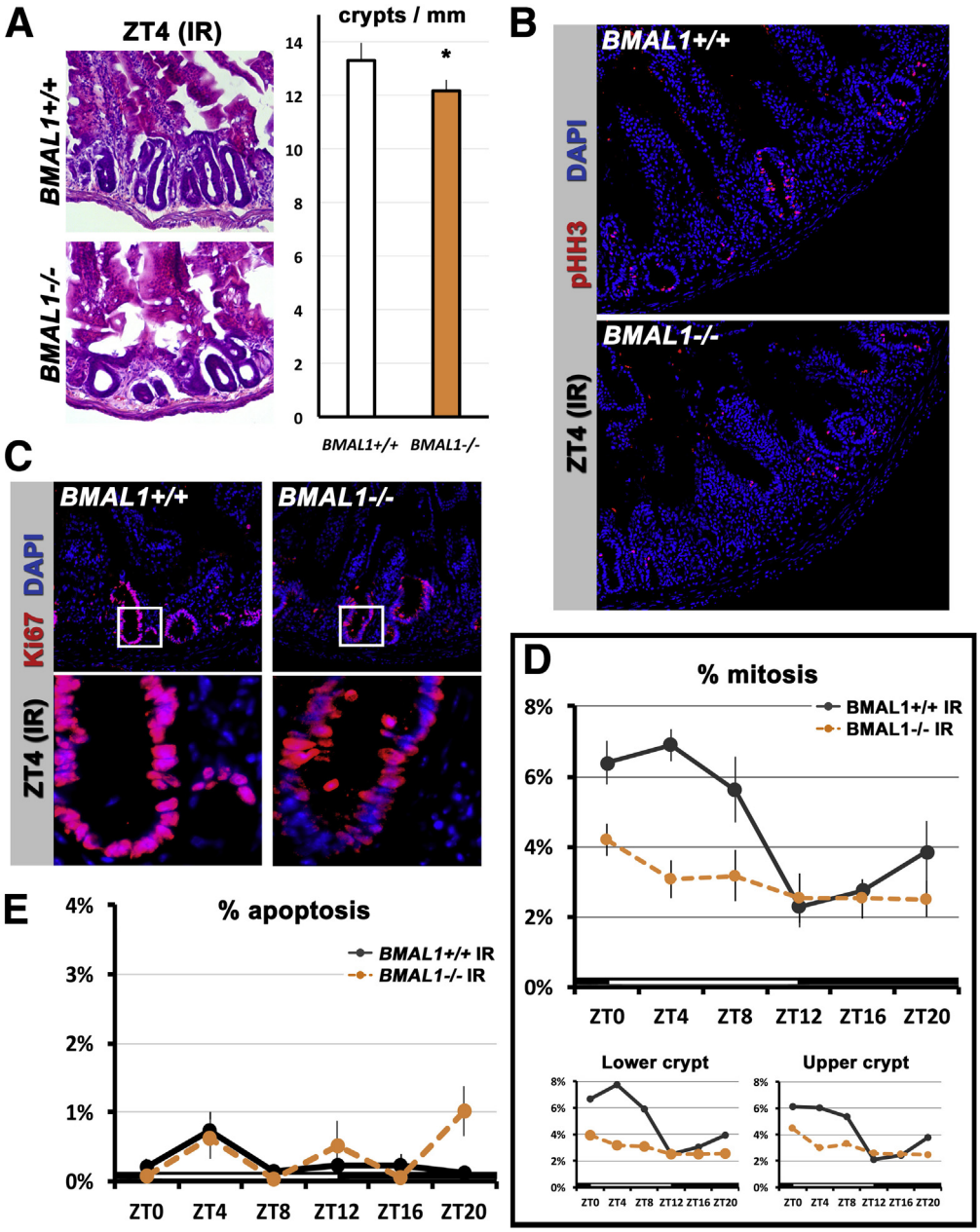

Figure 2. A *BMAL1*-dependent diurnal rhythm is present during intestinal regeneration 4–5 days after injury. (*A*) Hematoxylin-eosin staining shows both *BMAL1*$^{+/+}$ and *BMAL1*$^{-/-}$ intestines are adversely affected during the gastrointestinal syndrome (compare with Figure 1*A*). The *BMAL1*$^{-/-}$ epithelium contains significantly fewer crypts ($P = .0272$). (*B*) Mitosis in the *BMAL1*$^{+/+}$ and $^{-/-}$ epithelium is marked by pHH3. Images show confocal stacks (merged) from 10-μm sections. (*C*) Cell proliferation (marked by Ki67, which labels cells in S/G2/M phases) is present in the irradiated (IR) intestine of both genotypes. *Insets* below first row of images show higher magnification of crypts that are proliferating. Images show single confocal sections of intestinal crypts. (*D*) The IR *BMAL1*$^{+/+}$ crypt has a diurnal rhythm in mitoses with significant differences at different times ($F = 7.30$; $P = .0002$). There are significant differences in mitoses between the *BMAL1*$^{+/+}$ and the *BMAL1*$^{-/-}$ crypt ($F = 19.07$; $P = .0002$). *BMAL1*$^{-/-}$ intestinal precursors proliferate arrhythmically and at a lower level overall than *BMAL1*$^{+/+}$. *Bottom panels* show that mitoses vary in both the lower half of crypts (transit-amplifying and stem cell region), and the upper half of crypts (transit-amplifying cell region). The first 24 hours of *BMAL1*$^{+/+}$ data are replotted from Figure 1*F*. (*E*) Cell death (marked by cleaved Caspase3, which labels cells undergoing apoptosis) shows no significant time-of-day differences in *BMAL1*$^{+/+}$ ($P = .5046$), or differences between *BMAL1*$^{+/+}$ and *BMAL1*$^{-/-}$ ($P = .1072$).

and 7*C*), 1-way analysis of variance to compare differences in time (Figures 1*B*–*E*, 3*B*, 4*A*, 4*C*, 5*B*, 6*A*, 6*B*, and 7*B*), and 2-way analysis of variance to compare difference in both genotype and time (or genotype and expression levels) (Figures 2*D*, 3*B*, 3*C*, 4*A*, 4*C*, 5*B*, 5*D*, 6*A*–*C*, 7*B*, 9*A*, and 9*B*). All statistics were done using Prism 5.0 software (Graphpad Software Inc). Results are indicated in legends; error bars show standard error of the mean.

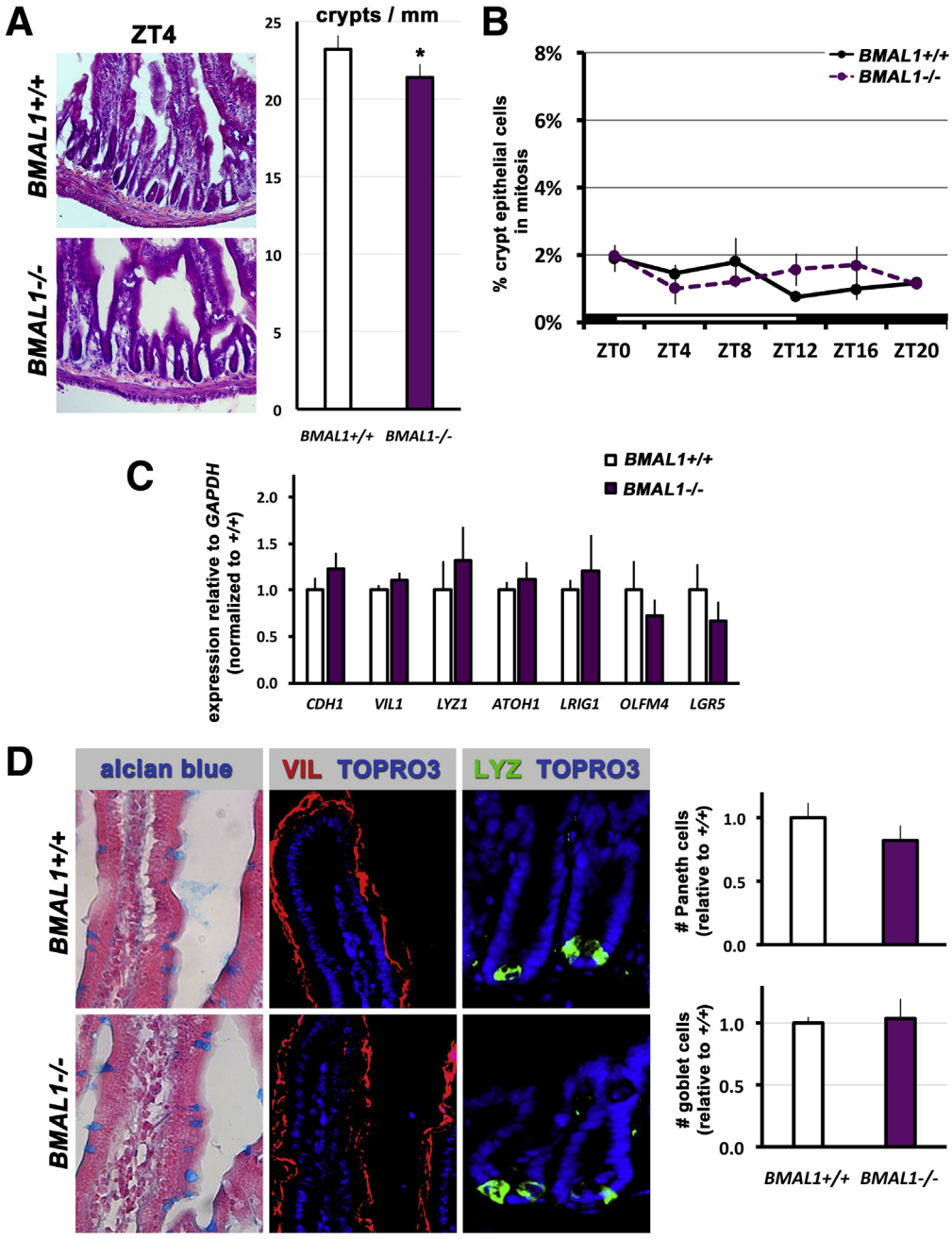

Figure 3. Loss of *BMAL1* produces no overt intestinal phenotypes in uninjured mice. (*A*) At 3 months of age the intestinal epithelium of *BMAL1*$^{-/-}$ mice resembles that of *BMAL1*$^{+/+}$ littermates. Hematoxylin-eosin staining shows similar crypt and villus morphology, although there is a significant difference in the number of crypts present ($P = .0076$). (*B*) Mitoses in the *BMAL1*$^{+/+}$ undamaged crypt epithelium show no significant diurnal variation ($P = .2909$), and there are no significant differences between *BMAL1*$^{+/+}$ and *BMAL1*$^{-/-}$ ($P = .6842$). The first 24 hours of *BMAL1*$^{+/+}$ data is replotted from Figure 1*E*. (*C*) Quantification of cell type markers by real-time quantitative polymerase chain reaction at ZT4 (n = 4 mice per genotype) shows no significant differences ($P = .7412$) in the expression of intestinal epithelial genes (*CDH1*, *VIL1*, *LYZ1*), and intestinal epithelial precursor and stem cell marker genes (*OLFM4*, *LRIG1*, *ATOH1*, *LGR5*). (*D*) The *BMAL1*$^{+/+}$ and *BMAL1*$^{-/-}$ epithelium shows the same number of goblet cells (alcian blue), enterocytes (VIL), and Paneth cells (LYZ) as shown by the presence of these cell-type markers. Brightfield images were taken using conventional microscopy, fluorescence images are confocal stacks (merged) from 10-μm sections taken. The number of Paneth cells, and goblet cells, is not significantly different between the 2 genotypes ($P = .2528$ and $P = .7950$, respectively).

Organoid Culture

Intestinal organoids were prepared and cultured from intestinal tissues of *BMAL1*$^{+/+}$, *BMAL1*$^{-/-}$, *BMAL1*$^{+/+}$;*FUCCI2*$^{+/-}$, *BMAL1*$^{-/-}$;*FUCCI2*$^{+/-}$, and *PER2-Luciferase* mice using established methods.[23] For timed RNA collection, and Luciferase experiments, organoids were passaged and grown for 3–4

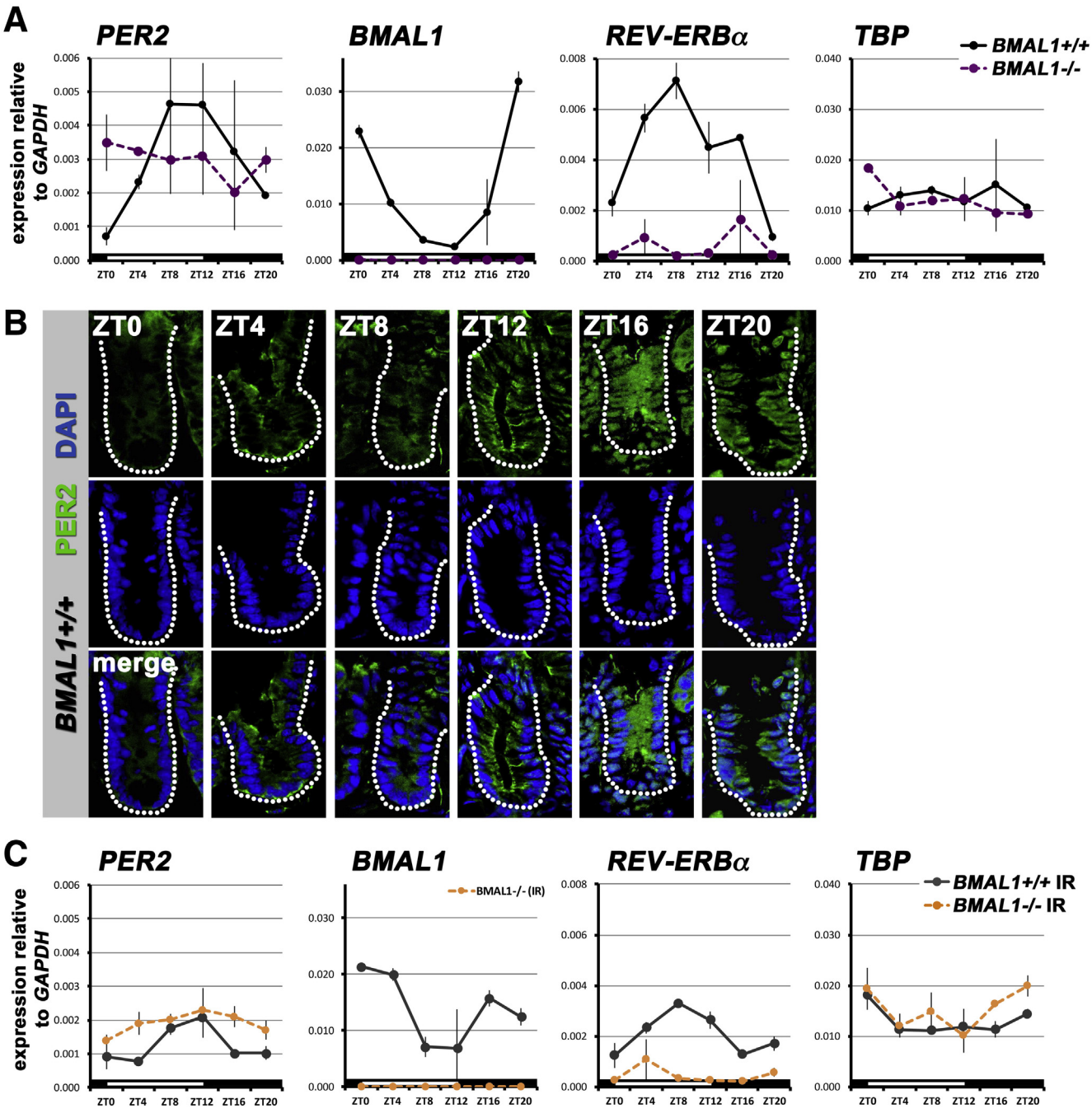

Figure 4. The intestinal epithelium displays a *BMAL1*-dependent circadian rhythm during normal homeostasis and during regeneration. (*A*) The *BMAL1*$^{+/+}$ intestine of animals on a standard 12-hour light/12-hour dark photoperiod shows rhythms in clock gene expression: *PER2* ($F = 7.267$; $P = .0055$), *BMAL1* ($F = 30.67$; $P < .0001$), and *REV-ERBα* ($F = 18.33$; $P = .0002$). *BMAL1*$^{-/-}$ animals do not show these rhythms: *PER2* ($P = .7839$), *BMAL1* ($P = .6397$), and *REV-ERBα* ($P = .6880$). Expression of the gene *TBP* (*TATA Binding Protein*) has no rhythm in either genotype. There are significant differences between genotypes in *PER2* ($F = 3.41$; $P = .0242$), *BMAL1* ($F = 219.0$; $P < .0001$), and *REV-ERBα* ($F = 87.27$; $P < .0001$). (*B*) PER2 protein is present in the undamaged intestinal precursors (crypts are outlined to indicate the region where precursors are located). PER2 is present in higher levels at ZT16–20, and shows nuclear localization in the epithelial cells of the crypt at these times. At ZT0–8, expression is weaker and predominantly cytoplasmic. Images show single confocal sections of intestinal crypts. (*C*) The 24-hour rhythm in clock gene expression 4 days after irradiation is similar to the undamaged intestine, but at lower levels relative to *GAPDH*. The gene TBP is not affected by the clock, or stress, and has no circadian rhythm. There are significant differences between genotypes in *PER2* ($F = 120.8$; $P < .0001$), *BMAL1* ($F = 225.7$; $P < .0001$), and *REV-ERBα* ($F = 74.65$; $P < .0001$). IR, irradiation.

days, then pulsed with 100 nM dexamethasone (Sigma) for 1 hour. Dexamethasone media was then replaced with fresh media. For RNA sampling, organoids were collected at 4-hour intervals from 0–28 hours (time is indicated in figures), by lysing directly into RLT buffer (Qiagen) with 1% β-mercaptoethanol. Figure 5*D* organoid RNA was collected from unsynchronized organoids, collected before passaging and untreated with dexamethasone. Bioluminescence recordings were performed after dexamethasone treatment, by adding Luciferin (Gold Biotechnologies) to organoid media at a final concentration of 0.1 mM and monitoring cultures for light output at 15-minute intervals using a Hamamatsu LM2400 bioluminescence recorder and Hamamatsu LM2400 software version 12. For tumor necrosis factor (TNF) experiments, organoids were grown for 6–8 days, then media containing 10 ng/mL recombinant TNF (Life Technologies), or 10 ng/mL recombinant TNF together with 100 ng/mL function blocking TNF antibody (R&D Systems, Minneapolis, MN), was applied for the indicated times (see figures). Organoids were not synchronized using dexamethasone in Figures 5*D* or 7, and "untreated" are organoids given new media (but with no TNF or anti-TNF) and collected at 24 hours. For staining and immunofluorescence, organoids were separated from Matrigel using Cell Recovery Solution (Corning, Canada) for 30 minutes on ice, and fixed for 1.5 hours in 4% PFA (EMS). For irradiation experiments (Figure 5*E*), organoids (unsynchronized/not treated with dexamethasone) were exposed to X-ray radiation at Day 3 of culture, at 0–8 Gy, then assayed by CellTiter Glo assay (Promega, Madison, WI) for cell number 4 days later. In all organoid experiments, 3–4 samples were examined per condition (genotype, and/or time point).

Western Blotting

Organoids were separated from Matrigel by incubating in Cell Recovery Solution (Corning) on ice for 30 minutes, supernatant was removed, and samples were lysed in RIPA buffer containing Pierce Protease and Phosphatase Inhibitor (Pierce, Toronto, Ontario, Canada). Electrophoresis was carried out on PAGEr EX Gels (Lonza, Basel, Switzerland) and Western blotted on PVDF (Thermo Scientific). Westerns were blocked 30 minutes with 5% milk in PBS-T 0.1% Triton X100. Primary antibodies were incubated overnight at 4°C: anti-Ki67 1:1000 (Abcam ab15580), anti-pJun S73 1:2000 (Cell Signaling Technology D47G9), and anti-Tubulin 1:5000 (Sigma). Secondary antibodies were incubated for 1 hour at room temperature: Dk anti-Rabbit-HRP or anti-Mouse-HRP 1:10000 (Jackson ImmunoResearch 711-35-152, 715-035-15, respectively). HRP was developed using Super Signal Femto (Thermo Scientific) and imaged on a FluorChem E Gel Imager (Protein Simple, San Jose, CA). Three samples were examined for each genotype at all time points indicated in the figures.

Results

Timing of Cell Death and Proliferation During the Gastrointestinal Syndrome

When intestinal cells are damaged and die, stem and precursor cells divide to replace cells and return the epithelium to its original state. Intuitively, this process would be facilitated if cells were produced as quickly as possible. To explore the timing of epithelial cell replacement, we investigated the small intestine of mice after high-dose (12 Gy) irradiation (Figure 1*A*). The number of proliferating cells was assessed using antibody to pHH3, which labels cells undergoing mitosis, and the number of dying cells was assessed using antibody to cleaved Caspase3, which labels cells undergoing apoptosis. Immediately following irradiation, proliferation is very low, then sharply increases as crypts disintegrate 1 day later (Figure 1*B*). We could not distinguish between proliferating epithelial cells or those from adjacent tissues, such as the blood system, because 1 day after irradiation the epithelium is highly morphologically disorganized. However, after this time epithelial proliferation gradually increases as crypts reappear and grow to regenerate the epithelium. These data are consistent with previous reports that have shown epithelial repair occurs several days after damage by irradiation.[6,24] In contrast to proliferation, apoptosis peaks 1 day after irradiation, but then decreases to low levels when crypts are proliferating (Figure 1*B*). We focused our investigation on 4–5 days following irradiation, when proliferation is at high levels and apoptosis is at lower levels.

The regenerating small intestine of mice with the gastrointestinal syndrome was compared with the intestine of unirradiated control animals. Analysis of overall crypt number showed a marked decrease during the gastrointestinal syndrome compared with control animals (13.3 ± 0.7 crypts per mm vs 23.2 ± 0.9 crypts per mm; Student's t test; $P < .0001$), presumably caused by extensive cell death from radiation.[5] However, unlike crypts in undamaged intestines whose cell number remains constant over the course of 24 hours (Figure 1*C*), the surviving crypts during the gastrointestinal syndrome are hyperplastic (Figure 1*D*), suggesting an increased rate of proliferation in response to damage.

To assess the mitotic index, we quantified the percentage of pHH3-positive nuclei relative to the total number of crypt nuclei present. During the gastrointestinal syndrome, the intestine shows a higher mitotic incidence than in control mice (Figures 1*E* and *F*), confirming the tissue is undergoing rapid regeneration. The nonirradiated intestine shows $\leq$2% mitotic cells in crypts over the course of 24 hours. Strikingly, the rate of mitoses during the gastrointestinal syndrome demonstrates a diurnal rhythm: the mitotic index at its peak is 5%–7% (ZT4) and at its lowest is 2%–3% (ZT12). This diurnal pattern of peaks and troughs repeats itself with a 24-hour period (Figure 1*F*), and mitoses are present in the upper and lower regions of the crypt suggesting that circadian regulation occurs in the stem cell and transit-amplifying cell populations. These results are consistent with studies published >40 years ago reporting daily variability in intestinal cell proliferation,[25,26] but which are now overlooked in studies of intestinal regeneration.

BMAL1 Is Required for Diurnal Proliferation Rhythms During the Gastrointestinal Syndrome

The circadian clock functions in nearly all cells of the body, including the stomach,[15] intestine,[14] and colon.[13,15] In

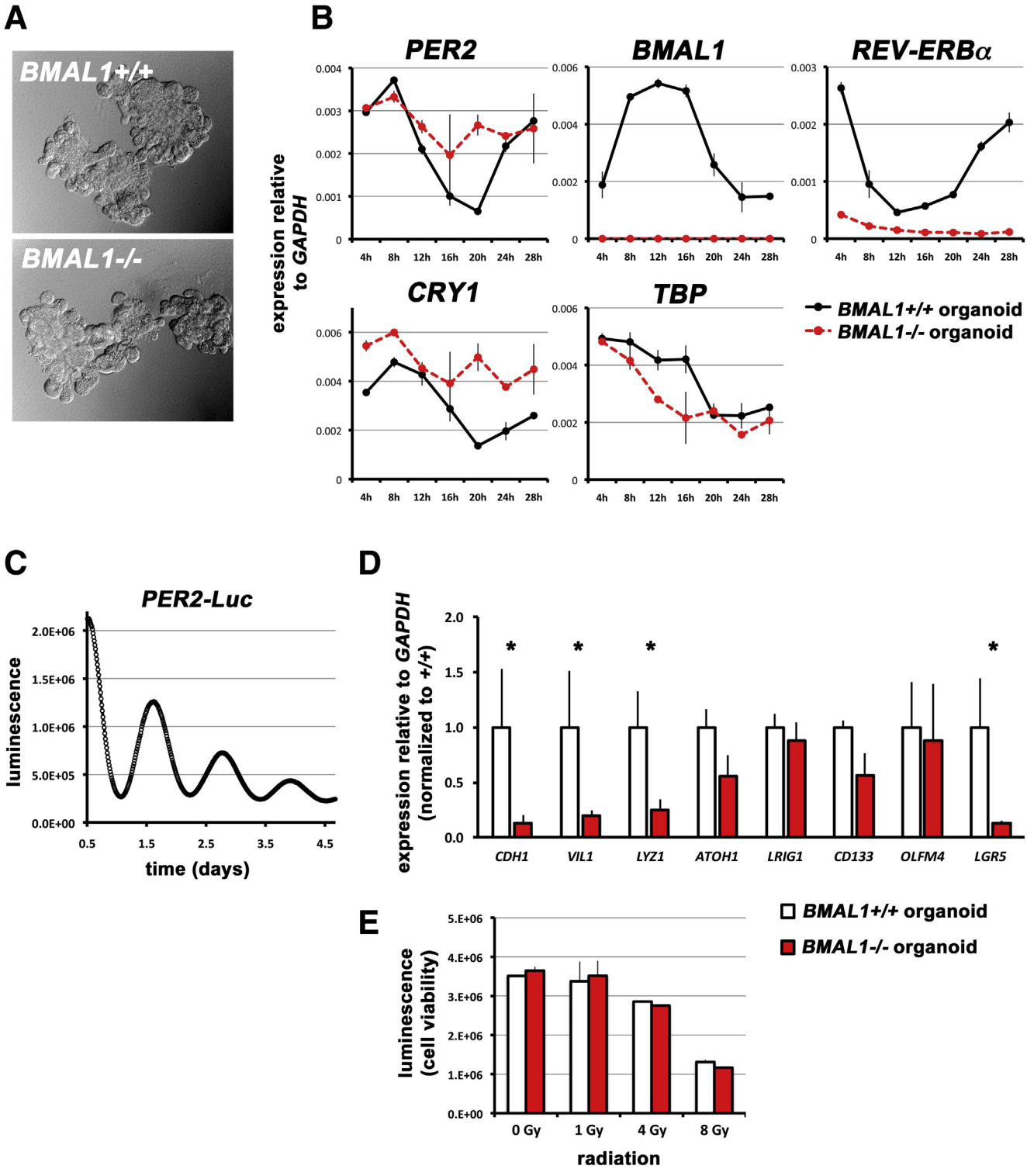

Figure 5. The intestinal epithelium has a clock. (*A*) Intestinal organoids were established from both *BMAL1*$^{+/+}$ and $^{-/-}$ intestines. Phase-contrast images are shown in brightfield. (*B*) *BMAL1*$^{+/+}$ organoids show circadian rhythms in clock gene expression: *PER2* ($F = 46.41$; $P < .0001$), *BMAL1* ($F = 38.41$; $P < .0001$), *REV-ERBα* ($F = 46.10$; $P < .0001$), and *CRY1* ($F = 15.96$; $P = .0009$). The control gene *TBP* does not show such rhythms but rather a gradual decrease following dexamethasone synchronization. There are significant differences between genotypes in *PER2* ($F = 5.21$; $P = .0387$), *BMAL1* ($F = 866.6$; $P < .0001$), *REV-ERBα* ($F = 556.8$; $P < .0001$), and *CRY1* ($F = 32.17$; $P < .0001$). (*C*) Organoids were established from 3 separate *PER2-Luc* intestines and luminescence readings show that rhythms in transcriptional clock activity persist for several days (1 representative tracing is shown). (*D*) Cellular markers in unsynchronized organoids quantified by real-time quantitative polymerase chain reaction show that *BMAL1*$^{-/-}$ intestinal organoids have decreased expression of *CDH1* ($P = .0148$), *VIL1* ($P = .0223$), *LYZ1* ($P = .0498$), and *LGR5* ($P = .0149$) expression. (*E*) The number of viable organoid cells (CellTiter Glo assay) is equivalent between *BMAL1*$^{+/+}$ and *BMAL1*$^{-/-}$ organoids, 4 days after varying doses of X-ray irradiation (as indicated in the graph). The intestinal epithelium has no significant BMAL1-dependent differences in sensitivity to radiation ($P = .5310$).

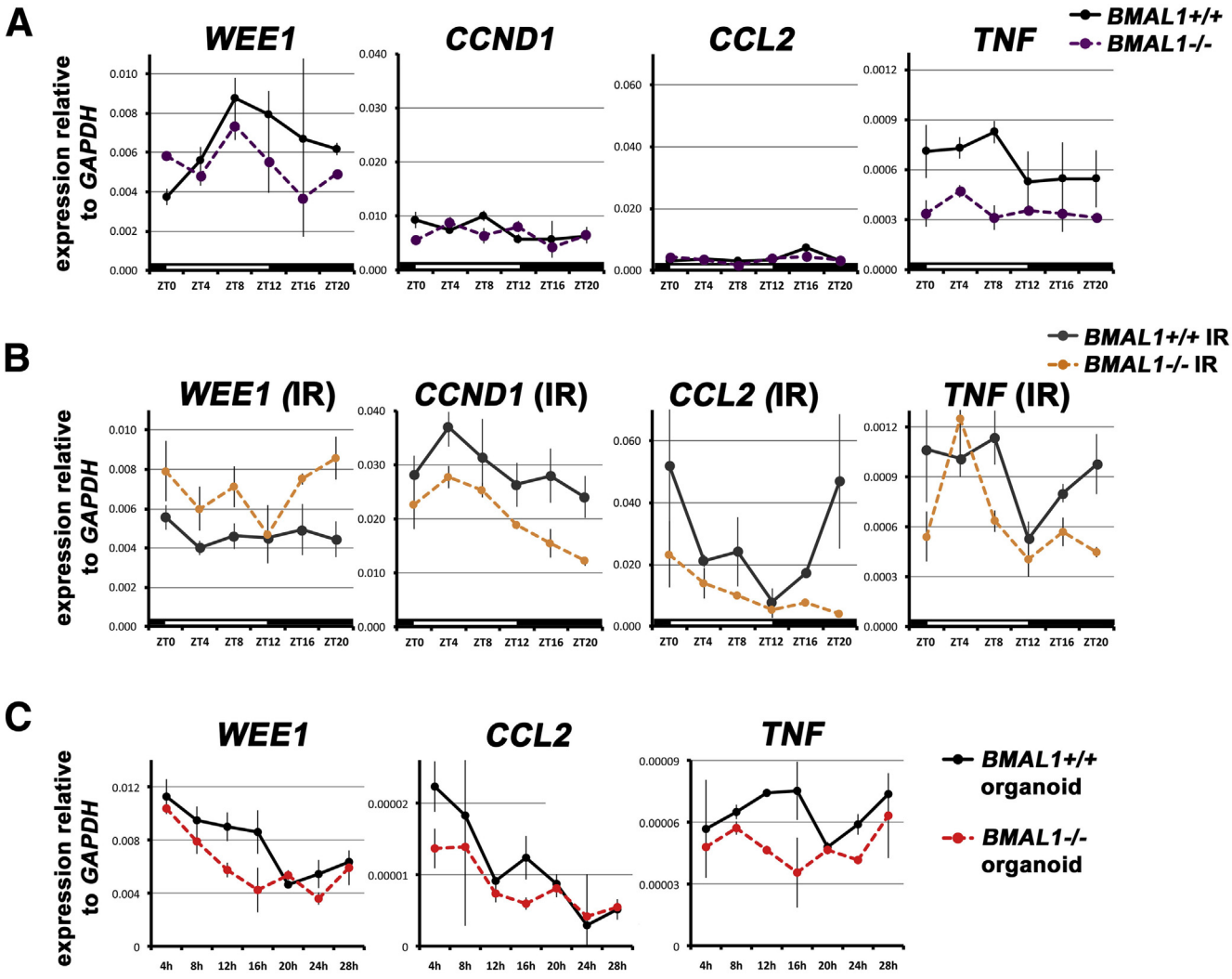

Figure 6. The regenerative response influences the 24-hour rhythms of genes. (*A*) *WEE1* shows diurnal variability in the undamaged intestine, with significant differences between *BMAL1*$^{+/+}$ and *BMAL1*$^{-/-}$ ($F = 8.04$; $P = .0005$). *CCND1* and *CCL2* expression are similar in both genotypes, whereas *TNF* exhibits 24-hour variability in the undamaged *BMAL1*$^{+/+}$ intestine, but none in the *BMAL1*$^{-/-}$ ($F = 15.99$; $P = .0008$). (*B*) During the gastrointestinal syndrome (IR), *WEE1* is arrhythmic ($P = .7382$), but *CCND1* displays high and low periods of expression over 24 hours. These are not likely a function of the circadian clock, but rather a response to environmental changes (eg, feeding), because the *BMAL1*$^{-/-}$ mutant also shows the same pattern, albeit at a significantly lower level ($F = 16.04$; $P = .0006$). *CCL2* exhibits a *BMAL1*-dependent circadian rhythm ($F = 4.318$; $P = .0176$), as does *TNF* ($F = 4.204$; $P = .0221$). There are significant differences between genotypes in *CCL2* ($F = 7.13$; $P = .0137$) and *TNF* ($F = 7.66$; $P = .0109$). Increased levels of *TNF* are present in *BMAL1*$^{-/-}$ mice at ZT4, whose levels are otherwise lower at all times compared with *BMAL1*$^{+/+}$. It is only at this time point that expression is elevated, suggesting that *TNF* production in the absence of *BMAL1* may be a response to an environmental cue (eg, feeding). (*C*) *BMAL1*$^{+/+}$ organoids show no rhythms in *WEE1* or *CCL2* expression (compare with the control gene *TBP* in Figure 5*B*); however, *TNF* is expressed with a 24-hour rhythm in *BMAL1*$^{+/+}$ but not *BMAL1*$^{-/-}$ organoids ($F = 10.45$; $P = .0060$). This suggests that only *TNF* is regulated by the clock in intestinal epithelial cells. IR, irradiation.

these gastrointestinal tissues, the clock has been proposed to play a key role in digestion and homeostasis[7,16]; however, its role in intestinal regeneration has not been studied genetically in mammals. We therefore investigated the core clock gene, *BMAL1*, using *BMAL1*$^{-/-}$ mutant mice that are viable but have a complete loss of circadian clock function.[9] *BMAL1*$^{-/-}$ mice have been shown to display signs of premature ageing, hence we performed all of our studies using mice at 12–15 weeks of age before ageing and other health-related phenotypes have been observed.[27] *BMAL1*$^{+/+}$ and *BMAL1*$^{-/-}$ littermate mice were housed on a 12-hour light/12-hour dark photoperiod to test the role of *BMAL1* in regeneration.

During the gastrointestinal syndrome both *BMAL1*$^{+/+}$ and *BMAL1*$^{-/-}$ intestines lose their characteristic morphology, and *BMAL1*$^{-/-}$ crypts show a ~10% decrease in abundance relative to *BMAL1*$^{+/+}$ (Figure 2*A*). Regenerating crypts of both genotypes are highly proliferative, as

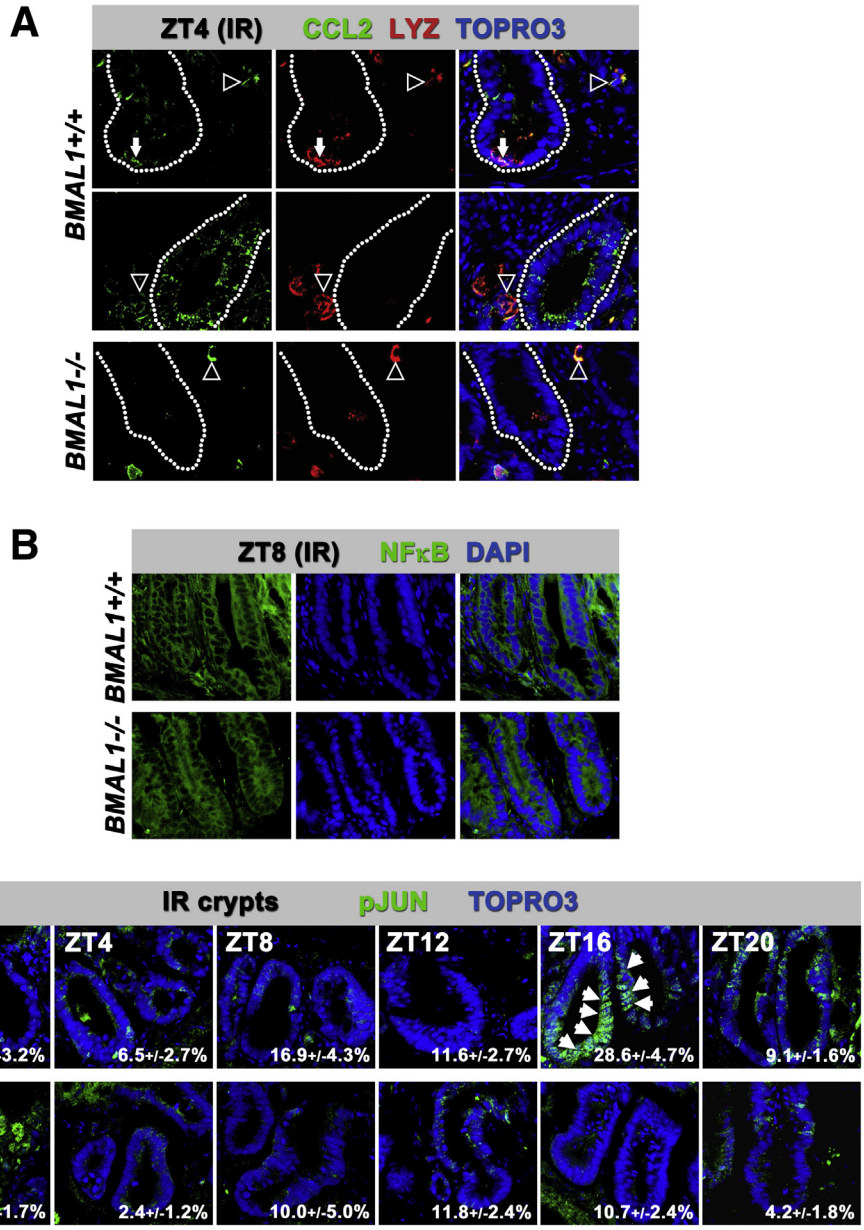

Figure 7. The circadian clock regulates JNK signaling. (*A*) CCL2 chemokine is expressed heterogenously in epithelial cells including LYZ^{+} Paneth cells (*arrows* in *top* row of images), and crypt precursors (epithelial cells within crypt shown in *middle* row of images), as well as blood cells that are likely monocytes or macrophages that, like Paneth cells, all coexpress *LYZ* (cells outside of crypts denoted by *arrowheads*). Images show confocal stacks (merged) from 10-μm sections taken at ZT4 (crypts are outlined). (*B*) The NFκB transcription factor does not show significant nuclear accumulation at any time point over 24 hours (ZT8 is shown as an example), in either genotype, suggesting it is not regulated by the circadian clock. (*C*) pJUN shown by its nuclear localization (*arrows*) is higher in *BMAL1*$^{+/+}$ crypts at ZT16–20 during the gastrointestinal syndrome. Although pJUN shows variability between crypts and within crypt cells, overall the *BMAL1*$^{-/-}$ intestine shows less activity at all times. Images show confocal stacks (merged) from 10-μm sections. Quantification of the percentage of pJUN^{+} crypt cells is indicated in the individual panels.

marked by the presence of antibody to pHH3, which labels cells in M-phase (Figure 2*B*), and Ki67, which labels cells in G1/S/G2/M-phases (Figure 2*C*). In contrast to the *BMAL1*$^{+/+}$ regenerating intestine, the mitotic index in the regenerating *BMAL1*$^{-/-}$ intestine does not show a diurnal rhythm (Figure 2*D*). Significant differences in mitosis are present between the *BMAL1*$^{+/+}$ and *BMAL1*$^{-/-}$ intestine, with the latter showing a lower mitotic index and arrhythmic cell production. However, unlike these proliferation differences, apoptosis is equivalent between the 2 genotypes and is not rhythmic (Figure 2*E*). These data show that diurnal, *BMAL1*-dependent changes in proliferation occur in the epithelium during the gastrointestinal syndrome, and that the loss of *BMAL1* causes a small decrease in overall crypt number.

BMAL1 *Is Not Required During Intestinal Tissue Maintenance in Uninjured Mice*

We next tested whether intestinal cell production is *BMAL1*-dependent under normal, undamaged conditions. The loss of *BMAL1* produced no obvious differences in intestinal crypt or villus morphology; however, a slight but significant decline in the number of crypts was noted (Figure 3*A*). This result is consistent with recent findings that the *PER1/PER2* double mutant also has a slight decrease in crypt number.[28] The *BMAL1*-related difference in baseline crypt number may explain the overall reduction in the number of crypts following irradiation (Figure 2*A*). In the absence of radiation damage, we found no significant diurnal variation in mitoses in the *BMAL1*$^{+/+}$ intestine, and no significant differences between *BMAL1*$^{+/+}$ and

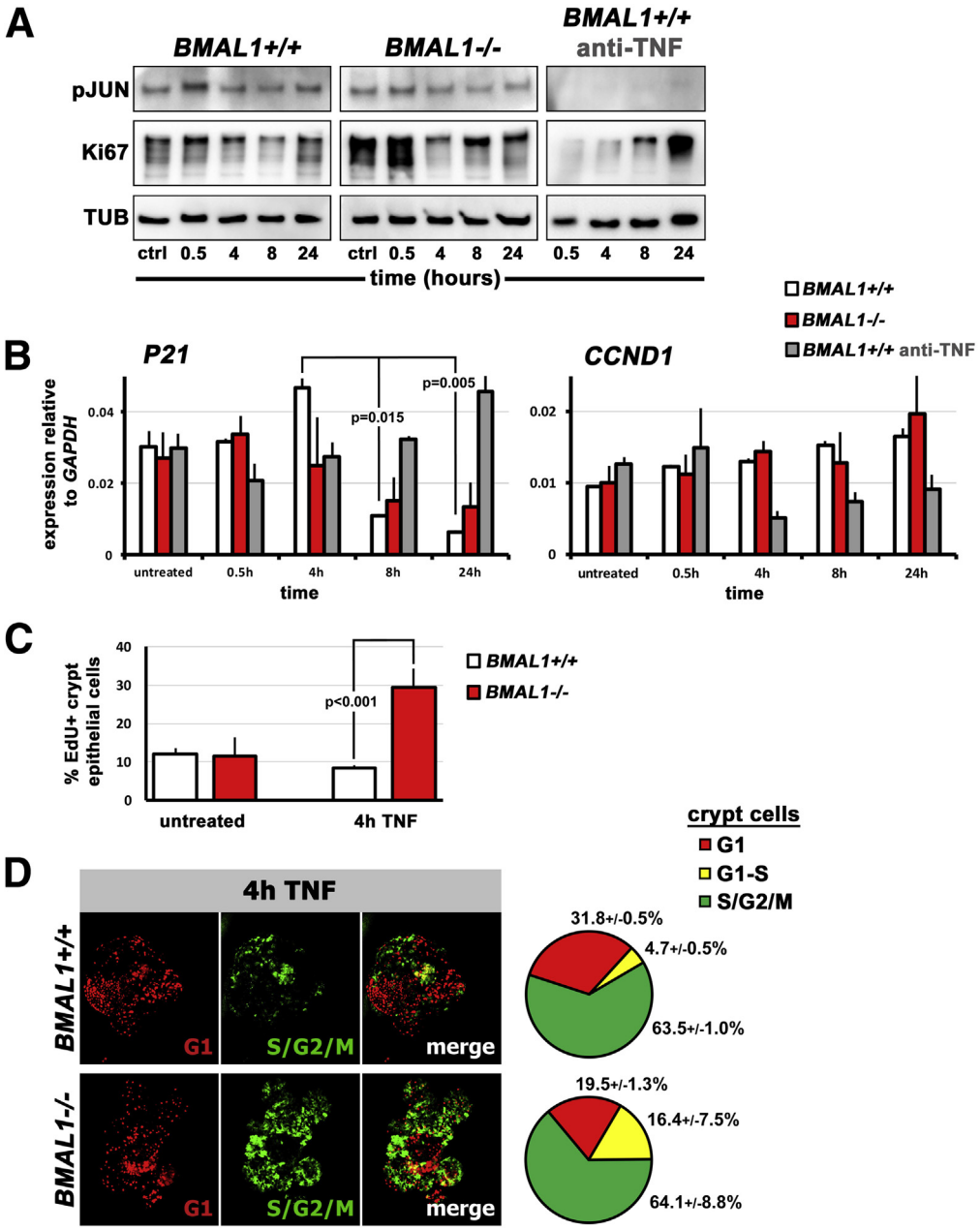

Figure 8. The circadian clock regulates proliferation timing in the intestinal epithelium. (*A*) Representative Western blots from 3 organoid lines examined per genotype (*outer black lines* indicate separate blots). *BMAL1*$^{+/+}$ intestinal organoids show a JNK signaling response to TNF at 0.5 hours (pJUN), which is absent when organoids are treated with anti-TNF inhibitor. TNF treated *BMAL1*$^{+/+}$ organoids are proliferative (Ki67), but this is also reduced by anti-TNF. *BMAL1*$^{-/-}$ organoids show a JNK (pJUN) response to TNF, but their proliferation (Ki67) is initially very high compared with *BMAL1*$^{+/+}$. (*B*) *BMAL1*$^{+/+}$ organoids exhibit a TNF-dependent upregulation of P21 expression ($F = 36.85$; $P = .0007$), with an initial increase at 4 hours followed by a sharp decrease at 8 hours (Tukey multiple comparisons test shown). *BMAL1*$^{-/-}$ do not show this pattern, and anti-TNF treatment of *BMAL1*$^{+/+}$ organoids results in an increase rather than decrease in *P21* expression over time. There are significant differences in *P21* between these genotypes/conditions ($F = 4.061$; $P = .0033$). Expression of the JUN target gene, *CCND1*, is significantly lowered by anti-TNF in BMAL1$^{+/+}$ organoids over time ($F = 9.865$; $P = .0017$) but does not vary significantly between *BMAL1*$^{+/+}$ and *BMAL1*$^{-/-}$ organoids ($P = .6678$). (*C*) S-phase (marked by EdU uptake) is higher in *BMAL1*$^{-/-}$ organoids 4 hours after TNF treatment, consistent with their lower level of P21 at this time (Student's *t* test comparison is shown). Untreated organoids (media change only) show no such differences ($P = .7811$). (*D*) The FUCCI cell cycle reporter shows that *BMAL1*$^{+/+}$ organoids have greater numbers of crypt cells in G1-phase compared with *BMAL1*$^{-/-}$ organoids, 4 hours after TNF induction. Pie charts show the percentage of crypt cells in each phase, in the corresponding genotypes; there are significantly more G1 cells in *BMAL1*$^{+/+}$ compared with *BMAL1*$^{-/-}$ (Student's *t* test, $P = .0020$).

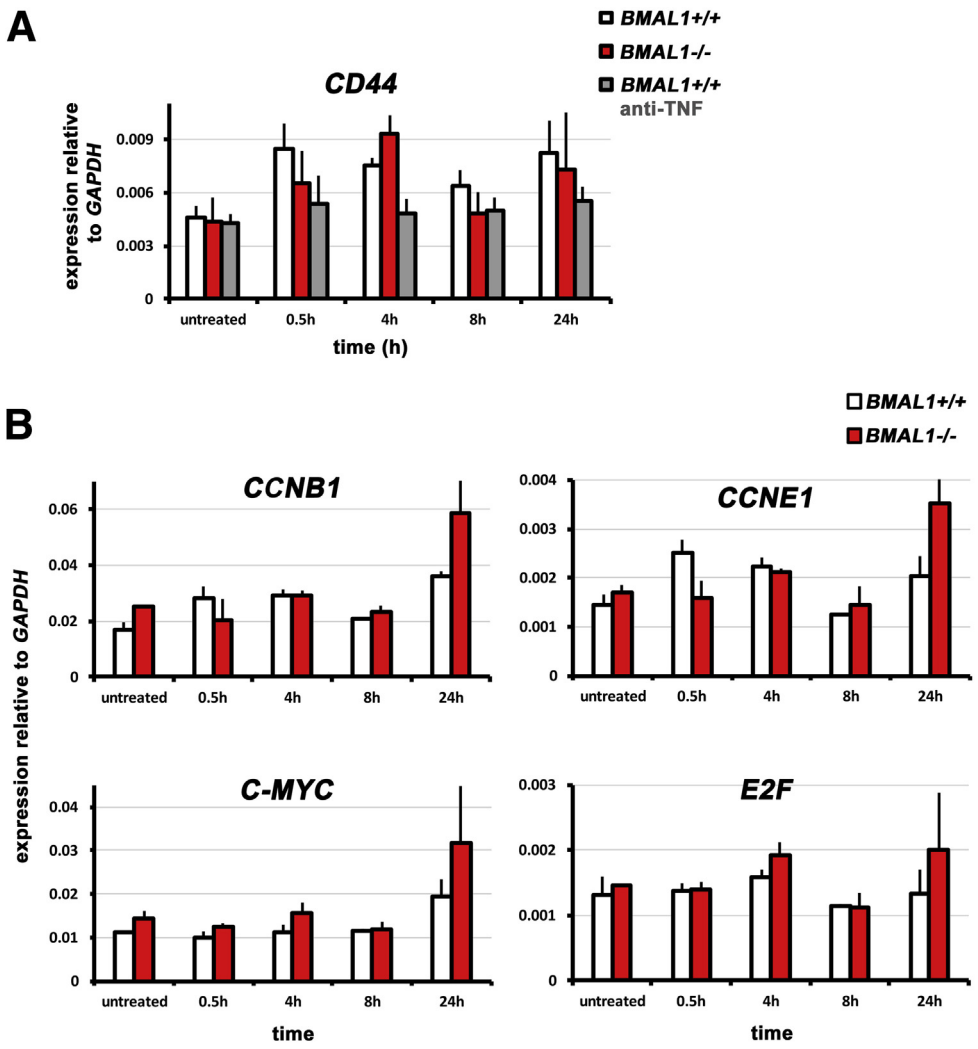

Figure 9. Equivalent gene expression in intestinal organoid culture. (*A*) *BMAL1*$^{+/+}$, *BMAL1*$^{-/-}$, and *BMAL1*$^{+/+}$ organoids treated with anti-TNF show similar expression of the JNK target gene *CD44* ($P = .8363$). (*B*) *BMAL1*$^{-/-}$ organoids show similar expression of the cell cycle regulators *CCNB1* ($P = .5970$), *CCNE1* ($P = .4307$), *C-MYC* ($P = .7082$), and *E2F* ($P = .8220$) when stimulated with TNF.

BMAL1$^{-/-}$ (Figure 3*B*). The absence of such rhythms in maintenance conditions is consistent with studies that reported no daily variation in intestinal cell production,[29,30] predating subsequent studies that reported a circadian rhythm.[25,26]

To assess the impact of BMAL1 loss on cell lineage development, intestine cell-specific markers were examined via quantitative real-time polymerase chain reaction between *BMAL1*$^{+/+}$ and *BMAL1*$^{-/-}$ mice. No significant differences in expression levels between the genotypes was found, suggesting that the epithelial cell lineage is intact when *BMAL1*$^{-/-}$ is absent (Figure 3*C*). However, we did note that *LGR5* and *OLFM4*, both markers of a crypt base stem cell population,[1] are slightly lower in *BMAL1*$^{-/-}$. No obvious differences in morphology or distribution in goblet cells, enterocytes, or Paneth cells were noted (Figure 3*D*), suggesting that the production of differentiated cells in the *BMAL1*$^{-/-}$ intestine is unaffected under baseline conditions. We further quantified Paneth cells and goblet cell numbers, and confirmed there were no significant differences between the *BMAL1*$^{+/+}$ and *BMAL1*$^{-/-}$ intestine (Figure 3*D*). We conclude that under maintenance conditions, the loss of *BMAL1* does not disrupt intestinal epithelial tissue renewal.

Circadian Clock Activity Persists During Stress

The intestine has been reported to exhibit 24-hour rhythms in clock gene expression,[14] hence we investigated the expression of circadian clock genes in the intestine of *BMAL1*$^{+/+}$ and *BMAL1*$^{-/-}$ littermate mice. Consistent with previous reports,[13–16,31] the undamaged intestine of *BMAL1*$^{+/+}$ mice exhibits a diurnal expression pattern of *PER2*, *BMAL1*, and *REV-ERBα* (Figure 4*A*). The sinusoidal, rhythmic expression profiles are consistent with rhythms seen in other mouse tissues, with *BMAL1* expression peaking at ZT20, approximately antiphase to the time of peaks of *PER2* (ZT8-12) and *REV-ERBα* (ZT8).[32] The *BMAL1*$^{-/-}$ intestine shows no rhythms in the expression of these genes under the same conditions, confirming the clock is dysfunctional when *BMAL1* is absent. The gene *TBP*, which is not clock-regulated,[33] shows no rhythms in either genotype under LD photoperiod.

Table 1. List of Primer Sequences

Target	Forward primer	Reverse primer
ATOH1	GAGTGGGCTGAGGTAAAAGAGT	GGTCGGTGCTATCCAGGAG
BMAL1	TGACCCTCATGGAAGGTTAGAA	GGACATTGCATTGCATGTTGG
CCL2	TTAAAAACCTGGATCGGAACCAA	GCATTAGCTTCAGATTTACGGGT
CCND1	GCGTACCCTGACACCAATCTC	CTCCTCTTCGCACTTCTGCTC
CCNE1	GTGGCTCCGACCTTTCAGTC	CACAGTCTTGTCAATCTTGGCA
CD133	CCTTGTGGTTCTTACGTTTGTTG	CGTTGACGACATTCTCAAGCTG
CD44	TCGATTTGAATGTAACCTGCCG	CAGTCCGGGAGATACTGTAGC
CDH1	TCGGAAGACTCCCGATTCAAA	CGGACGAGGAAACTGGTCTC
C-MYC	ATGCCCCTCAACGTGAACTTC	GTCGCAGATGAAATAGGGCTG
CRY1	CACTGGTTCCGAAAGGGACTC	CTGAAGCAAAAATCGCCACCT
E2F	GAGAAGTCACGCTATGAAACCTC	CCCAGTTCAGGTCAACGACAC
GAPDH	AGGTCGGTGTGAACGGATTTG	TGTAGACCATGTAGTTGAGGTCA
LGR5	CCTACTCGAAGACTTACCCAGT	GCATTGGGGTGAATGATAGCA
LRIG1	TTGAGGACTTGACGAATCTGC	CTTGTTGTGCTGCAAAAAGAGAG
LYZ1	GAGACCGAAGCACCGACTATG	CGGTTTTGACATTGTGTTCGC
OLFM4	CAGCCACTTTCCAATTTCACTG	GCTGGACATACTCCTTCACCTTA
P21	CCTGGTGATGTCCGACCTG	CCATGAGCGCATCGCAATC
PER2	GAAAGCTGTCACCACCATAGAA	AACTCGCACTTCCTTTTCAGG
REV-ERBα	TGAACGCAGGAGGTGTGATTG	GAGGACTGGAAGCTATTCTCAGA
TBP	AGAACAATCCAGACTAGCAGCA	GGGAACTTCACATCACAGCTC
TNF	CCCTCACACTCAGATCATCTTCT	GCTACGACGTGGGCTACAG
VIL1	TCAAAGGCTCTCTCAACATCAC	AGCAGTCACCATCGAAGAAGC
WEE1	GAAACAAGACCTGCCAAAAGAA	GCATCCATCTAACCTCTTCACAC

We next examined PER2 protein in intestinal crypts by immunofluorescence over a 24-hour time span (Figure 4*B*). PER2 protein is rhythmically expressed under circadian clock regulation, in many tissues, with a peak abundance that typically lags behind maximal transcript levels by 4–6 hours.[34] In the intestine, PER2 is expressed at higher levels during the night (ZT16-20), in the crypts where proliferating intestinal stem cells and transit-amplifying cells reside.

To assess if the circadian clock continues to function during the pathologic state of the gastrointestinal syndrome, we tested the expression of *BMAL1*, *PER2*, and *REV-ERBα* transcripts. These clock genes exhibit diurnal rhythms in $BMAL1^{+/+}$ mice that peak at times similar to the undamaged intestine, but are reduced in levels relative to *GAPDH* (Figure 4*C*). Thus, the circadian clock is intact during the intestinal regenerative response, and shows similar activity timing as during normal conditions (Figure 4*A*). These data suggest that the gastrointestinal syndrome does not reset the phase of the intestinal clock.

Circadian Clock Regulates Intestinal Organoid Gene Expression

The intestine contains epithelium, muscle, nerves, blood cells, and connective tissues, and the clock transcripts detected in our samples (Figures 3*C*, 4*A*, and 4*C*) may be expressed by any of these cells. Previous circadian studies have relied on similar sampling methods,[15,16] or have enriched for differentiated epithelial cells by scraping them from the surrounding tissues.[13,14] Although scraping enriches for epithelial genes, samples may contain non-epithelial cell RNA. To specifically assess the circadian clock in the intestinal epithelium, we established pure epithelial cell cultures using intestinal stem cells from $BMAL1^{+/+}$ and $BMAL1^{-/-}$ mice to generate organoids (Figure 5*A*).[23]

Organoids were treated with a 1-hour pulse of dexamethasone to synchronize their clocks,[33] resulting in rhythmic expression of the clock genes *BMAL1*, *PER2*, *CRY1*, and *REV-ERBα* (Figure 5*B*). $BMAL1^{+/+}$ intestinal organoids show clock gene expression patterns (Figure 5*B*) that strongly resemble those *in vivo* (Figure 4), whereas $BMAL1^{-/-}$ do not, suggesting that the intestinal epithelium contains a functional circadian system that requires BMAL1. The control gene *TBP is* not rhythmic in organoids, and displays a gradual decrease in expression over this time. We further confirmed that intestinal organoids express tissue-autonomous circadian rhythms by examining bioluminescence rhythms in organoids derived from *PER2-Luciferase* mice.[35] *Per2-Luciferase* organoids show circadian rhythms that persist for >4 days following synchronization (Figure 5*C*). These results are consistent with recent reports using organoid culture,[28,36] which support that the intestinal epithelium has a tissue-autonomous, *BMAL1*-dependent circadian clock.

We next reexamined the expression of cell-specific markers to test the consequence of BMAL1 loss in organoid culture. We examined organoids before dexamethasone synchronization, and compared $BMAL1^{+/+}$ and $BMAL1^{-/-}$ at

1 time point (Figure 5*D*). Quantitative real-time polymerase chain reaction showed that *BMAL1*$^{-/-}$ organoids have lower expression of the differentiated genes *CDH1*, *VIL1*, and *LYZ1*, as well as *LGR5*, a marker of intestinal precursor and stem cells. These deficiencies suggest that the production or function of epithelial cells is autonomously reduced in the intestinal epithelium, when *BMAL1* is absent. To further test cell production in organoids, we examined cell number in organoids in normal conditions, and 4 days following exposure to 1, 4, or 8 Gy X-irradiation. There were no significant *BMAL1*-dependent differences in organoid cell number assayed following irradiation damage (Figure 5*E*). Our results are consistent with previous findings that the circadian clock does not regulate cell survival *in vitro* following irradiation.[37]

Cell Cycle Regulators Are Arrhythmic During Regeneration

Cell division often exhibits a 24-hour cycle but how or whether it is linked to the circadian clock is a matter of long-standing research.[10] Two cell cycle regulators, *WEE1* and *CCND1*, have been previously implicated as clock targets,[38,39] and we therefore hypothesized that these might drive rhythms in cell proliferation during the gastrointestinal syndrome.

WEE1 is a direct CLK/BMAL1 target in the liver, where it represses the G2-M phase transition.[38] In the undamaged *BMAL1*$^{+/+}$ intestine, *WEE1* expression has a diurnal rhythm (peak is ZT8-12), consistent with previous reports,[14] and its expression in *BMAL1*$^{-/-}$ animals is arrhythmic, suggesting clock control (Figure 6*A*). However, at this time point mitoses are not actually rhythmic (Figure 3*B*). During the gastrointestinal syndrome, *WEE1* expression is arrhythmic (Figure 6*B*), despite the strong diurnal rhythm in mitosis present (Figure 2*D*). This suggests *WEE1* rhythms are decoupled from proliferation rhythms in this tissue, hence, we further tested whether the intestinal epithelial clock regulates *WEE1* autonomously using organoid culture. Despite possessing circadian clock activity (Figures 5*B* and *C*), *BMAL1*$^{+/+}$ organoids do not exhibit rhythms in *WEE1* gene expression (Figure 6*C*).

CCND1 (*CyclinD*) is regulated by CLK/BMAL1 in osteoblasts, where it enables the G1-S phase transition.[40] *CCND1* is arrhythmic in both the *BMAL1*$^{+/+}$ and *BMAL1*$^{-/-}$ intestine under normal conditions (Figure 6*A*), but exhibits 24-hour variation during the gastrointestinal syndrome (Figure 6*B*). This daily pattern of *CCND1* expression is similar in both the *BMAL1*$^{+/+}$ and *BMAL1*$^{-/-}$ intestine, suggesting it is not regulated by the circadian clock. Taken together, these data suggest that neither *WEE1* nor *CCND1* link the clock and the cell cycle in the intestinal epithelium. We therefore sought to investigate other mechanisms that could shed light on how the epithelium proliferates with a circadian rhythm.

Cytokine Production Is Rhythmic During Regeneration

The immune system has circadian rhythms[41,42] as evidenced by its highly variable time-of-day-dependent response to infection,[43,44] its susceptibility to photoperiod disruption,[45] and clock regulation of cytokine production.[42–44] Inflammation is likely to affect intestinal physiology during the gastrointestinal syndrome, and recently it has been shown that the innate immune system coordinates circadian rhythms between the microbiota and the intestinal epithelium.[46] We therefore examined whether inflammation during the gastrointestinal syndrome regulates intestinal cell production. The immune system produces many factors whose rhythmic expression could drive circadian processes in the epithelium. We tested the expression of several cytokines (*TNF*, *IL6*, *IL10*, *IL17B*, *IL22*, and *CCL2*), some of which have been previously implicated in the circadian biology of the immune system.[41–43]

CCL2, a chemokine that recruits monocytes to regions of infection and injury, is not expressed with diurnal variation in the undamaged intestine (Figure 6*A*), but shows diurnal changes during the gastrointestinal syndrome in *BMAL1*$^{+/+}$ but not in *BMAL1*$^{-/-}$ (Figure 6*B*). The *TNF* cytokine displays diurnal variation in *BMAL1*$^{+/+}$ intestines during normal conditions, and is arrhythmic and lower in *BMAL1*$^{-/-}$ (Figure 6*A*). During the gastrointestinal syndrome, the *BMAL1*$^{+/+}$ intestine exhibits diurnal changes in *TNF*. These are altered in *BMAL1*$^{-/-}$ animals, which show a single sharp peak at ZT4, but otherwise remain lower than *BMAL1*$^{+/+}$ at all other times (Figure 6*B*). These results suggest that *TNF* and *CCL2* exhibit clock-dependent expression during the gastrointestinal syndrome. The interleukin genes we examined (*IL6*, *IL10*, *IL17B*, and *IL22*) did not show any diurnal *BMAL1*-dependent changes under the 2 conditions examined.

We tested whether *TNF* and *CCL2* are produced by the intestinal epithelium. *TNF* is known to be expressed in intestinal epithelial cells,[47] and *BMAL1*$^{+/+}$ organoids exhibit 24-hour rhythms in *TNF* that are absent in *BMAL1*$^{-/-}$ organoids, suggesting it is a clock target in the epithelium (Figure 6*C*). *CCL2* is not expressed with a rhythm in organoid culture (Figure 6*C*), suggesting its rhythmic expression *in vivo* is not caused by the epithelium. This was further tested by antibody staining in irradiated animals, where *CCL2* was expressed by cells that stained positively for the marker LYZ, suggesting these were monocytes or macrophages (Figure 7*A*). *CCL2* was also expressed in the epithelium at ZT4 in both epithelial precursors and Paneth cells where it is has been shown to be induced by TNF.[48] These results suggest that CCL2 is produced by both the epithelium and resident white blood cells, but that epithelial cells are not responsible for *CCL2* diurnal rhythms during the gastrointestinal syndrome.

BMAL1 *Regulates the Tumor Necrosis Factor Response*

TNF is an inflammatory cytokine, which can signal through both NFκB and c-JUN transcription factors.[49] These pathways have been recently implicated in intestinal proliferation: sustained activity of NFκB[50] or JNK[51] leads to hyperplasia and tumorigenesis. We tested the activity of the TNF pathway by staining for NFκB and pJUN over a 24-hour

time course, 4 days following radiation injury. NFκB is predominantly cytoplasmic in the crypt cells of both *BMAL1*$^{+/+}$ and *BMAL1*$^{-/-}$ mice, suggesting that NFκB is not active under these conditions (Figure 7*B*). In contrast, pJUN has a higher nuclear signal in the proliferating crypts of *BMAL1*$^{+/+}$ mice at ZT16, during the gastrointestinal syndrome, but is lower at other times (Figure 7*C*). *BMAL1*$^{-/-}$ crypts show lower signal and no diurnal variation over 24 hours. This suggests JNK signaling is regulated by the circadian clock during the gastrointestinal syndrome, either through rhythmic production of TNF by the surrounding myeloid cells[42] or from epithelial cells themselves (Figure 6*C*).

Signaling between intestinal epithelial and nonepithelial cells is a very complex dynamic. Hence we tested whether *BMAL1* regulates the epithelial response to TNF using intestinal organoids, which contain only epithelial cells. Both *BMAL1*$^{+/+}$ and *BMAL1*$^{-/-}$ organoids have an immediate response to TNF, which causes an increase in pJUN levels 0.5 hours after stimulation (Figure 8*A*). Function-blocking anti-TNF antibody completely abolishes the pJUN response in *BMAL1*$^{+/+}$ organoids confirming this is a TNF-dependent process. We next examined a possible link between TNF signaling and proliferation. *BMAL1*$^{+/+}$ organoids are proliferative (Ki67 positive) before and after TNF-stimulation, suggesting TNF does not reduce epithelial proliferation during inflammation. In contrast, Ki67 is initially much higher in *BMAL1*$^{-/-}$ organoids and decreases 4 hours after TNF exposure. Function-blocking anti-TNF antibody reduces Ki67 expression, showing that TNF promotes proliferation in the epithelium. Together, these data show that *BMAL1* regulates cell proliferation downstream of TNF, but the JNK pathway is *BMAL1*-independent.

JUN target genes, in particular cell cycle and cell growth regulators, were examined during TNF activation. *BMAL1*$^{-/-}$ organoids have equivalent expression of the JUN target genes *CCND1* and *CD44*, but show differences in the regulation of *P21* (also called *CDKN1A*), a negative regulator of proliferation (Figures 8*B* and 9*A*). Specifically, *BMAL1*$^{+/+}$ organoids exhibit a TNF-dependent upregulation of *P21* expression 4 hours after induction followed by a sharp decrease at 8 hours. This response is completely absent in *BMAL1*$^{-/-}$ organoids, which simply show a gradual decrease in *P21* expression. This suggests the timing of cell cycle entry, during an inflammatory response, is altered when *BMAL1* is absent. However, the altered expression of cell cycle regulators is not a general feature of *BMAL1*$^{-/-}$ organoids, because these show equivalent expression of *CCNB1*, *CCNE1*, *E2F*, and *C-MYC* (Figure 9*B*). We hypothesized that 1 function of *BMAL1* is to produce a ~4-hour delay in cell cycle entry during the regenerative response to TNF.

To test this hypothesis, we assessed the number of epithelial cells undergoing S-phase using EdU labeling in *BMAL1*$^{+/+}$ versus *BMAL1*$^{-/-}$ organoids following TNF treatment. *BMAL1*$^{+/+}$ organoids, whose *P21* levels are higher, show reduced S-phase entry compared with *BMAL1*$^{-/-}$ organoids, whose levels of *P21* are lower at this time (Figure 8*C*). To further assess the impact of TNF on cell cycle dynamics, we crossed the *FUCCI2* cell cycle reporter strain,[52] which marks cells in G1 (RFP) and S/G2/M (GFP), on the *BMAL1* background. We generated organoids from the *BMAL1*$^{+/+}$, *FUCCI2*$^{+/-}$ versus *BMAL1*$^{-/-}$, *FUCCI2*$^{+/-}$ mice and tested their response to TNF treatment. Consistent with their increase in S-phase entry, *BMAL1*$^{-/-}$ organoid cells show a decrease in G1 phase compared with *BMAL1*$^{+/+}$ control animals (Figure 8*D*). These data show that 1 function of *BMAL1* is to regulate the timing of cell proliferation in response to inflammatory stress. Not only does the clock regulate *TNF* expression itself (Figures 6*A*–*C*), but in response to TNF, the circadian clock regulates the timing of epithelial S-phase.

Discussion

We find that the circadian clock is active in the intestinal epithelium during normal and pathologic states. However, these distinct physiological states exhibit differences in circadian gene expression. Epithelial regeneration during the gastrointestinal syndrome shows circadian rhythms in proliferation, and cytokines and cell cycle regulators are regulated by the core clock gene *BMAL1*. These outputs are not present in the undamaged state, suggesting this program is dynamically initiated during regeneration. Based on these data, we propose a model of circadian clock function in the small intestine in which the targets TNF and P21 cooperate to drive diurnal rhythms in cell production (Figure 10).

Circadian Proliferation in the Intestinal Epithelium

The intestine has been reported to exhibit circadian rhythms in its physiology, including 24-hour rhythms in proliferation.[7,25,26] However, we found no significant diurnal changes in mitosis under normal homeostatic conditions in this tissue (Figure 1*E*). Similarly, early attempts to find circadian rhythms in the small intestine were also unsuccessful.[29,30,53] There are several possibilities to account for these discrepancies. Previous studies that reported circadian rhythms in mitoses[25] may have sampled different regions of the small intestine, which exhibit regional differences in circadian clock activity.[14] For instance, such regions as the duodenum show very slight diurnal changes in S-phase versus such regions as the ileum that show high-amplitude changes.[7] It is possible the regions we sampled (ie, the duodenum and proximal jejunum) do not show high-amplitude 24-hour changes under undamaged conditions. Another possibility is that specific phases of the cell cycle might be differentially regulated by the clock, or other factors, such as diet and/or microbiota, could also affect the expression of intestinal rhythmicity.

Despite the absence of mitotic rhythms during normal conditions, we find strong diurnal variation in mitosis during the regenerative response following irradiation (Figure 1*F*). Because studies supporting[7,25,26] and refuting[29,30,53] circadian rhythmicity in intestinal cell proliferation have been published, it is also possible that an additional factor contributes to these rhythms. Reports of circadian rhythms in the digestive tract applied tritiated thymidine to label cells undergoing S-phase.[25,26] These

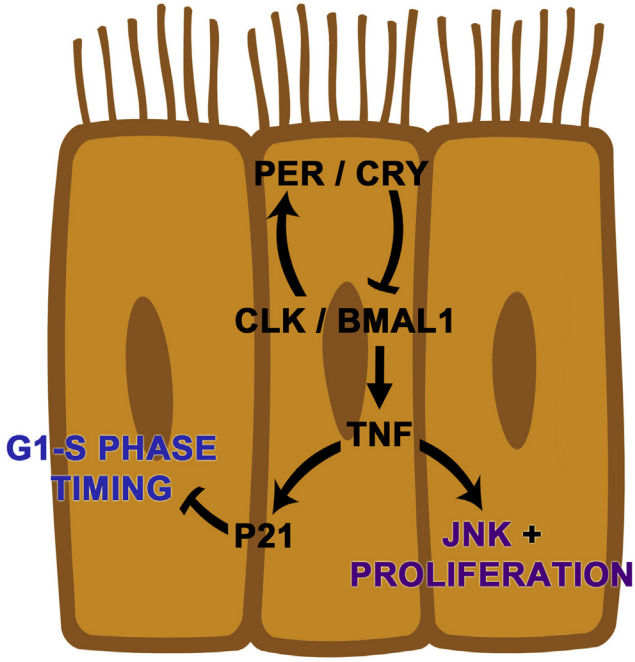

Figure 10. A proposed model of circadian clock function in the regenerating small intestinal epithelium. *BMAL1* controls *TNF* and *P21* during a pathologic state. TNF cytokine signaling increases epithelial proliferation in epithelial precursors to replace damaged epithelial cells. Rhythms in TNF production may arise from the epithelium but also are well known to be rhythmically produced by the immune system (see discussion). In epithelial cells, P21 response is under clock control downstream of TNF to regulate diurnal rhythms in cell production.

experiments involved injecting animals over a 24-hour timeline and collecting samples $\geq$1 hour after injection. To avoid an injection-related stress response, we assayed the cell cycle noninvasively by detecting M-phase using antibody to pHH3, and detected diurnal rhythms in cell production during a pathologic state. We have previously shown that proliferation in the *Drosophila* intestine is gated by the circadian clock only during regeneration, and that before damage no rhythms are detected.[54] This bears a similarity to our present results, and we thus suggest physiological stresses drive and/or amplify circadian rhythms in cell proliferation.

Circadian Control of the Cell Cycle

There is compelling evidence to link the cell cycle with the circadian clock,[10] and regulators, such as *WEE1*, have been shown to be *bona fide* clock targets in the liver.[38] A direct link between cell cycle regulation and the circadian clock has yet to be established in the intestinal epithelium. A recent study has shown that cell proliferation rhythms in the colon can be changed by altering the timing of food intake,[31] suggesting the clock may not control the cell cycle in intestinal epithelia directly. We find that *WEE1* is arrhythmic during healing (Figure 6*B*), when proliferation is rhythmic (Figure 2*D*), demonstrating that the cell cycle and the clock are either not directly linked, or can be decoupled. Our results support that the circadian clock controls the cell cycle regulator *P21*, during the inflammatory response to TNF. Twenty-four-hour rhythms in the expression of *P21* have been observed in cancer patient colon biopsies suggesting this finding may be conserved in mammals.[55]

In addition to these connections, we cannot discount circadian control of the cell cycle through transcriptional or posttranscriptional regulation of different genes involved in proliferation. Genome-wide transcriptome and proteome analysis of all cell cycle regulators in this tissue would resolve this question, and the precise targeting of cell cycle regulators by the circadian clock in the intestinal epithelium.

Circadian Control of Cell Signaling

Genes involved in the immune response, such as *TNF* and *CCL2*, exhibit diurnal rhythms during healing. In particular, the *TNF* inflammatory cytokine exhibits diurnal changes in the intestine (Figures 6*A* and *B*) and is rhythmically expressed in organoid epithelia autonomously (Figure 6*C*). TNF production has been shown to exhibit circadian rhythms in a variety of tissues,[42,43] and it is very likely to be produced by the epithelium and its surrounding cells. A recent study showed that the regulation of *TNF* expression in the colon is disrupted in clock mutants exposed to alcohol-induced injury.[56] This suggests the role of the clock in the regulation of these genes may be a general feature in digestive tract pathology. Further work is needed to resolve the complex interplay between clock-regulated sources of the different cytokines that regulate the digestive system.

Similar to our previous studies in *Drosophila*,[54] proliferation rhythms during regeneration involve signaling processes. Overall, our results suggest that as epithelial cells switch from a state of tissue maintenance to a state of regeneration, the circadian clock regulates different target genes. Such a process may involve the recruitment of transcriptional regulators to work in conjunction with the genes *CLK* and *BMAL1*, *REV-ERBα*, or *RORα* in the same cell. Alternatively, context-dependent posttranscriptional mechanisms[11,57] may alter transcriptional output in these cells during regeneration.

The effect of cytokines on epithelial cell production is particularly relevant in understanding how disease states, such as inflammation and cancer, are related.[58] *TNF* is of particular importance and, consistent with our results, has been recently reported to increase the proliferation of intestinal organoids.[59] *TNF* can activate both NFκB[50] and JNK[51,60] pathways, both of which promote proliferation and tumorigenesis of intestinal epithelia. We find that *TNF* is produced rhythmically by the intestinal epithelium under clock control, and that the clock further regulates the proliferation response to TNF. The DNA-binding activity of JUN has been observed to be circadian,[46] consistent with these findings. Our results showing the circadian clock regulation of *P21* are consistent with observations in the circadian expression of *P21* in human[55] and zebrafish[61]

cells, overall suggesting a conserved mechanism of cell cycle control.

JNK signaling can enhance Wnt pathway activity in the intestinal epithelium,[51] and *cJUN* has also been shown to be enriched in the LGR5^{+} intestinal stem cell population.[62] NFκB activation also enhances Wnt signaling and causes the dedifferentiation of transit-amplifying cells into intestinal stem cells.[63] The rhythmic production of TNF in the epithelium during the gastrointestinal syndrome could therefore influence stem cell and transit-amplifying cells by boosting Wnt signaling. Similar circadian clock activity in stem cells has been documented in several systems.[64] In intestinal organoids, we find that the *BMAL1*$^{-/-}$ epithelium shows deficiencies in the expression of epithelial markers (Figure 5*D*). In particular, a reduction in *LYZ1* and *LGR5* expression in organoids may explain why the *BMAL1*$^{-/-}$ intestine shows a slight reduction in crypt number (Figures 2*A* and 3*A*) and LGR5 expression (Figure 3*C*) *in vivo*. LGR5^{+} intestinal stem cells are intermingled with Paneth cells in a Wnt signaling milieu, and a reduction in stem cell and Paneth cell markers suggests a maintenance deficiency. Although these phenotypes seem to be generally compensated during maintenance *in vivo* (Figure 3) and *in vitro* (Figure 5*E*), the circadian clock may play a role in epithelial Wnt signaling in certain physiological contexts. While this study was under revision, it was reported that Wnt signaling is regulated by the clock in intestinal organoids, caused by the expression of *WNT3A* by Paneth cells.[28] Circadian control of intestinal signaling pathways may be an important mechanism linking tissue homeostasis with general physiology.

Circadian Rhythms in Disease

The health of shift-workers who undergo photoperiod disruption is significantly worsened,[17–19] and our findings that rhythmic gene expression is *BMAL1*-dependent shows the circadian clock regulates important processes in the pathologic state. This highlights the underappreciated role of 24-hour timing in gastrointestinal illness, and future studies need to be done to test connections between photoperiod and disease etiology and progression. Although our work has been carried out in LD photoperiod where environmental light could induce diurnal changes that are not a direct function of clock activity, because we observe diurnal changes in the *BMAL1*$^{+/+}$ intestine that are not present in *BMAL1*$^{-/-}$, the effects we report are unlikely to be a simple response to environmental change. Our data highlight the importance of photoperiod on the mechanisms underlying disease. Current treatment regimens may be able to apply these and future insights from circadian biology.[65] Moreover, it will be critical to account for circadian rhythmicity, and time-of-day dependency, in the use of animal models to study the biology and treatment of gastrointestinal disease.

References

1. Medema JP, Vermeulen L. Microenvironmental regulation of stem cells in intestinal homeostasis and cancer. Nature 2011;474:318–326.
2. Metcalfe C, Kljavin NM, Ybarra R, de Sauvage FJ. Lgr5+ stem cells are indispensable for radiation-induced intestinal regeneration. Cell Stem Cell 2014;14:149–159.
3. Tian H, Biehs B, Warming S, Leong KG, Rangell L, Klein OD, de Sauvage FJ. A reserve stem cell population in small intestine renders Lgr5-positive cells dispensable. Nature 2011;478:255–259.
4. Dubois A, Walker RI. Prospects for management of gastrointestinal injury associated with the acute radiation syndrome. Gastroenterology 1988;95:500–507.
5. Kirsch DG, Santiago PM, di Tomaso E, Sullivan JM, Hou WS, Dayton T, Jeffords LB, Sodha P, Mercer KL, Cohen R, Takeuchi O, Korsmeyer SJ, Bronson RT, Kim CF, Haigis KM, Jain RK, Jacks T. p53 controls radiation-induced gastrointestinal syndrome in mice independent of apoptosis. Science 2010;327:593–596.
6. Somosy Z, Horvath G, Telbisz A, Réz G, Pálfia Z. Morphological aspects of ionizing radiation response of small intestine. Micron 2002;33:167–178.
7. Scheving LA. Biological clocks and the digestive system. Gastroenterology 2000;119:536–549.
8. Masri S, Sassone-Corsi P. The circadian clock: a framework linking metabolism, epigenetics and neuronal function. Nat Rev Neurosci 2013;14:69–75.
9. Bunger MK, Wilsbacher LD, Moran SM, Clendenin C, Radcliffe LA, Hogenesch JB, Simon MC, Takahashi JS, Bradfield CA. Mop3 is an essential component of the master circadian pacemaker in mammals. Cell 2000;103:1009–1017.
10. Borgs L, Beukelaers P, Vandenbosch R, Belachew S, Nguyen L, Malgrange B. Cell "circadian" cycle: new role for mammalian core clock genes. Cell Cycle 2009;8:832–837.
11. Koike N, Yoo SH, Huang HC, Kumar V, Lee C, Kim TK, Takahashi JS. Transcriptional architecture and chromatin landscape of the core circadian clock in mammals. Science 2012;338:349–354.
12. Zhang R, Lahens NF, Ballance HI, Hughes ME, Hogenesch JB. A circadian gene expression atlas in mammals: Implications for biology and medicine. Proc Natl Acad Sci U S A 2014;111:16219–16224.
13. Sladek M, Rybova M, Jindrakova Z, Zemanová Z, Polidarová L, Mrnka L, O'Neill J, Pácha J, Sumová A. Insight into the circadian clock within rat colonic epithelial cells. Gastroenterology 2007;133:1240–1249.
14. Polidarova L, Sotak M, Sladek M, Pacha J, Sumová A. Temporal gradient in the clock gene and cell-cycle checkpoint kinase Wee1 expression along the gut. Chronobiol Int 2009;26:607–620.
15. Hoogerwerf WA, Hellmich HL, Cornelissen G, Halberg F, Shahinian VB, Bostwick J, Savidge TC, Cassone VM. Clock gene expression in the murine gastrointestinal tract: endogenous rhythmicity and effects of a feeding regimen. Gastroenterology 2007;133:1250–1260.
16. Hoogerwerf WA, Sinha M, Conesa A, Luxon BA, Shahinian VB, Cornélissen G, Halberg F, Bostwick J, Timm J, Cassone VM. Transcriptional profiling of mRNA expression in the mouse distal colon. Gastroenterology 2008;135:2019–2029.

17. Caruso CC, Lusk SL, Gillespie BW. Relationship of work schedules to gastrointestinal diagnoses, symptoms, and medication use in auto factory workers. Am J Ind Med 2004;46:586–598.
18. Segawa K, Nakazawa S, Tsukamoto Y, Kurita Y, Goto H, Fukui A, Takano K. Peptic ulcer is prevalent among shift workers. Dig Dis Sci 1987;32:449–453.
19. Schernhammer ES, Laden F, Speizer FE, Willett WC, Hunter DJ, Kawachi I, Fuchs CS, Colditz GA. Night-shift work and risk of colorectal cancer in the nurses' health study. J Natl Cancer Inst 2003;95:825–828.
20. Preuss F, Tang Y, Laposky AD, Arble D, Keshavarzian A, Turek FW. Adverse effects of chronic circadian desynchronization in animals in a "challenging" environment. Am J Physiol Regul Integr Comp Physiol 2008; 295:R2034–R2040.
21. Shukla P, Gupta D, Bisht SS, Pant MC, Bhatt ML, Gupta R, Srivastava K, Gupta S, Dhawan A, Mishra D, Negi MP. Circadian variation in radiation-induced intestinal mucositis in patients with cervical carcinoma. Cancer 2010;116:2031–2035.
22. Reppert SM, Weaver DR. Coordination of circadian timing in mammals. Nature 2002;418:935–941.
23. Sato T, Clevers H. Primary mouse small intestinal epithelial cell cultures. Methods Mol Biol 2013;945:319–328.
24. Montgomery RK, Carlone DL, Richmond CA, Farilla L, Kranendonk ME, Henderson DE, Baffour-Awuah NY, Ambruzs DM, Fogli LK, Algra S, Breault DT. Mouse telomerase reverse transcriptase (mTert) expression marks slowly cycling intestinal stem cells. Proc Natl Acad Sci U S A 2011;108:179–184.
25. Sigdestad CP, Bauman J, Lesher SW. Diurnal fluctuations in the number of cells in mitosis and DNA synthesis in the jejunum of the mouse. Exp Cell Res 1969; 58:159–162.
26. Potten CS, Al-Barwari SE, Hume WJ, Searle J. Circadian rhythms of presumptive stem cells in three different epithelia of the mouse. Cell Tissue Kinet 1977;10:557–568.
27. Kondratov RV, Kondratova AA, Gorbacheva VY, Vykhovanets OV, Antoch MP. Early aging and age-related pathologies in mice deficient in BMAL1, the core component of the circadian clock. Genes Dev 2006; 20:1868–1873.
28. Matsu-Ura T, Dovzhenok A, Aihara E, Rood J, Le H, Ren Y, Rosselot AE, Zhang T, Lee C, Obrietan K, Montrose MH, Lim S, Moore SR, Hong CI. Intercellular coupling of the cell cycle and circadian clock in adult stem cell culture. Mol Cell 2016;64:900–912.
29. Leblond CP, Stevens CE. The constant renewal of the intestinal epithelium in the albino rat. Anat Rec 1948; 100:357–377.
30. Bertalanffy FD. Mitotic rates and renewal times of the digestive tract epithelia in the rat. Acta Anat (Basel) 1960; 40:130–148.
31. Yoshida D, Aoki N, Tanaka M, Aoyama S, Shibata S. The circadian clock controls fluctuations of colonic cell proliferation during the light/dark cycle via feeding behavior in mice. Chronobiol Int 2015:1–11.
32. Punia S, Rumery KK, Yu EA, Lambert CM, Notkins AL, Weaver DR. Disruption of gene expression rhythms in mice lacking secretory vesicle proteins IA-2 and IA-2beta. Am J Physiol Endocrinol Metab 2012; 303:E762–E776.
33. Balsalobre A, Marcacci L, Schibler U. Multiple signaling pathways elicit circadian gene expression in cultured Rat-1 fibroblasts. Curr Biol 2000;10:1291–1294.
34. Lee C, Etchegaray JP, Cagampang FR, Loudon AS, Reppert SM. Posttranslational mechanisms regulate the mammalian circadian clock. Cell 2001;107:855–867.
35. Yoo SH, Yamazaki S, Lowrey PL, Shimomura K, Ko CH, Buhr ED, Siepka SM, Hong HK, Oh WJ, Yoo OJ, Menaker M, Takahashi JS. PERIOD2::LUCIFERASE real-time reporting of circadian dynamics reveals persistent circadian oscillations in mouse peripheral tissues. Proc Natl Acad Sci U S A 2004;101:5339–5346.
36. Moore SR, Pruszka J, Vallance J, Aihara E, Matsuura T, Montrose MH, Shroyer NF, Hong CI. Robust circadian rhythms in organoid cultures from PERIOD2::LUCIFERASE mouse small intestine. Dis Model Mech 2014;7:1123–1130.
37. Gaddameedhi S, Reardon JT, Ye R, Ozturk N, Sancar A. Effect of circadian clock mutations on DNA damage response in mammalian cells. Cell Cycle 2012; 11:3481–3491.
38. Matsuo T, Yamaguchi S, Mitsui S, Emi A, Shimoda F, Okamura H. Control mechanism of the circadian clock for timing of cell division in vivo. Science 2003; 302:255–259.
39. Fu L, Pelicano H, Liu J, Huang P, Lee C. The circadian gene Period2 plays an important role in tumor suppression and DNA damage response in vivo. Cell 2002; 111:41–50.
40. Fu L, Patel MS, Bradley A, Wagner EF, Karsenty G. The molecular clock mediates leptin-regulated bone formation. Cell 2005;122:803–815.
41. Curtis AM, Bellet MM, Sassone-Corsi P, O'Neill LA. Circadian clock proteins and immunity. Immunity 2014; 40:178–186.
42. Keller M, Mazuch J, Abraham U, Eom GD, Herzog ED, Volk HD, Kramer A, Maier B. A circadian clock in macrophages controls inflammatory immune responses. Proc Natl Acad Sci U S A 2009;106, 21407–21012.
43. Bellet MM, Deriu E, Liu JZ, Grimaldi B, Blaschitz C, Zeller M, Edwards RA, Sahar S, Dandekar S, Baldi P, George MD, Raffatellu M, Sassone-Corsi P. Circadian clock regulates the host response to Salmonella. Proc Natl Acad Sci U S A 2013;110:9897–9902.
44. Gibbs JE, Blaikley J, Beesley S, Matthews L, Simpson KD, Boyce SH, Farrow SN, Else KJ, Singh D, Ray DW, Loudon AS. The nuclear receptor REV-ERBalpha mediates circadian regulation of innate immunity through selective regulation of inflammatory cytokines. Proc Natl Acad Sci U S A 2012;109:582–587.
45. Castanon-Cervantes O, Wu M, Ehlen JC, Paul K, Gamble KL, Johnson RL, Besing RC, Menaker M, Gewirtz AT, Davidson AJ. Dysregulation of inflammatory responses by chronic circadian disruption. J Immunol 2010;185:5796–5805.
46. Mukherji A, Kobiita A, Ye T, Chambon P. Homeostasis in intestinal epithelium is orchestrated by the circadian

clock and microbiota cues transduced by TLRs. Cell 2013;153:812–827.
47. Chen LW, Egan L, Li ZW, Greten FR, Kagnoff MF, Karin M. The two faces of IKK and NF-kappaB inhibition: prevention of systemic inflammation but increased local injury following intestinal ischemia-reperfusion. Nat Med 2003;9:575–581.
48. Lau KS, Cortez-Retamozo V, Philips SR, Pittet MJ, Lauffenburger DA, Haigis KM. Multi-scale in vivo systems analysis reveals the influence of immune cells on TNF-alpha-induced apoptosis in the intestinal epithelium. PLoS Biol 2012;10:e1001393.
49. Wajant H, Pfizenmaier K, Scheurich P. Tumor necrosis factor signaling. Cell Death Differ 2003;10:45–65.
50. Vlantis K, Wullaert A, Sasaki Y, Schmidt-Supprian M, Rajewsky K, Roskams T, Pasparakis M. Constitutive IKK2 activation in intestinal epithelial cells induces intestinal tumors in mice. J Clin Invest 2011; 121:2781–2793.
51. Sancho R, Nateri AS, de Vinuesa AG, Aguilera C, Nye E, Spencer-Dene B, Behrens A. JNK signalling modulates intestinal homeostasis and tumourigenesis in mice. EMBO J 2009;28:1843–1854.
52. Abe T, Sakaue-Sawano A, Kiyonari H, Shioi G, Inoue K, Horiuchi T, Nakao K, Miyawaki A, Aizawa S, Fujimori T. Visualization of cell cycle in mouse embryos with Fucci2 reporter directed by Rosa26 promoter. Development 2013;140:237–246.
53. Pilgrim C, Erb W, Maurer W. Diurnal fluctuations in the numbers of DNA synthesizing nuclei in various mouse tissues. Nature 1963;199:863.
54. Karpowicz P, Zhang Y, Hogenesch JB, Emery P, Perrimon N. The circadian clock gates the intestinal stem cell regenerative state. Cell Rep 2013;3:996–1004.
55. Griniatsos J, Michail OP, Theocharis S, Arvelakis A, Papaconstantinou I, Felekouras E, Pikoulis E, Karavokyros I, Bakoyiannis C, Marinos G, Bramis J, Michail PO. Circadian variation in expression of G1 phase cyclins D1 and E and cyclin-dependent kinase inhibitors p16 and p21 in human bowel mucosa. World J Gastroenterol 2006;12:2109–2114.
56. Summa KC, Jiang P, Fitzpatrick K, Voigt RM, Bowers SJ, Forsyth CB, Vitaterna MH, Keshavarzian A, Turek FW. Chronic alcohol exposure and the circadian clock mutation exert tissue-specific effects on gene expression in mouse hippocampus, liver, and proximal colon. Alcohol Clin Exp Res 2015;39:1917–1929.
57. Rey G, Cesbron F, Rougemont J, Reinke H, Brunner M, Naef F. Genome-wide and phase-specific DNA-binding rhythms of BMAL1 control circadian output functions in mouse liver. PLoS Biol 2011;9:e1000595.
58. Karin M, Clevers H. Reparative inflammation takes charge of tissue regeneration. Nature 2016;529:307–315.
59. Tattoli I, Killackey SA, Foerster EG, Molinaro R, Maisonneuve C, Rahman MA, Winer S, Winer DA, Streutker CJ, Philpott DJ, Girardin SE. NLRX1 acts as an epithelial-intrinsic tumor suppressor through the modulation of TNF-mediated proliferation. Cell Rep 2016;14:2576–2586.
60. Nateri AS, Spencer-Dene B, Behrens A. Interaction of phosphorylated c-Jun with TCF4 regulates intestinal cancer development. Nature 2005;437:281–285.
61. Laranjeiro R, Tamai TK, Peyric E, Krusche P, Ott S, Whitmore D. Cyclin-dependent kinase inhibitor p20 controls circadian cell-cycle timing. Proc Natl Acad Sci U S A 2013;110:6835–6840.
62. van der Flier LG, van Gijn ME, Hatzis P, Kujala P, Haegebarth A, Stange DE, Begthel H, van den Born M, Guryev V, Oving I, van Es JH, Barker N, Peters PJ, van de Wetering M, Clevers H. Transcription factor achaete scute-like 2 controls intestinal stem cell fate. Cell 2009; 136:903–912.
63. Schwitalla S, Fingerle AA, Cammareri P, Nebelsiek T, Göktuna SI, Ziegler PK, Canli O, Heijmans J, Huels DJ, Moreaux G, Rupec RA, Gerhard M, Schmid R, Barker N, Clevers H, Lang R, Neumann J, Kirchner T, Taketo MM, van den Brink GR, Sansom OJ, Arkan MC, Greten FR. Intestinal tumorigenesis initiated by dedifferentiation and acquisition of stem-cell-like properties. Cell 2013;152:25–38.
64. Brown SA. Circadian clock-mediated control of stem cell division and differentiation: beyond night and day. Development 2014;141:3105–3111.
65. Gumz ML. Taking into account circadian rhythm when conducting experiments on animals. Am J Physiol Renal Physiol 2016;310:F454–F455.

Received November 29, 2016. Accepted March 24, 2017.

Correspondence
Address correspondence to: Phillip Karpowicz, PhD, Department of Biological Sciences, University of Windsor, Windsor, Ontario, Canada N9B 3P4. e-mail: Phillip.Karpowicz@uwindsor.ca.

Acknowledgments
The authors thank Robert Montgomery, Alessio Tovaglieri, Samantha Stewart, Diana Carlone, Fanny Zhou, and Lijie Jiang for their technical support and valuable input, and Jennifer Gommerman and Dana Philpott for their help with the manuscript. The contents of this article are solely the responsibility of the authors and may not represent the official views of the sponsoring agencies.

Author contributions
Kyle Stokes performed experiments and contributed to writing. Abrial Cooke and Hanna Chang performed experiments. David R. Weaver performed and analyzed experiments and contributed to writing. David T. Breault designed the study and contributed to writing. Phillip Karpowicz designed the study, performed and analyzed experiments, and contributed to writing.

Conflicts of interest
The authors disclose no conflicts.

Funding
Kyle Stokes was funded by the Canadian Institutes of Health Research. David R. Weaver was supported by the National Institutes of Health (R01NS056125 and R21ES024684). David T. Breault was supported by the National Institutes of Health (R01DK084056), the Intellectual and Developmental Disabilities Research Center (P30HD18655), the Harvard Digestive Disease Center (P30DK034854), and the Timothy Murphy Fund. Phillip Karpowicz was funded by the Human Frontier in Science Program, the University of Windsor, and the Seeds4Hope/Windsor Cancer Foundation. The FUCCI2 reporter mouse strain was generously provided by the RIKEN Center for Life Science Technologies (Yokohama, Japan).